Jolie, E., Scott, S., Faulds, J., Chambefort, I., Axelsson, G., Gutiérrez-Negrín, L. C., Regenspurg, S., Ziegler, M., Ayling, B., Richter, A., Zemedkun, M. T. (2021): Geological controls on geothermal resources for power generation. - Nature Reviews Earth & Environment, 2, 324-339.

https://doi.org/10.1038/s43017-021-00154-y

Geological controls on geothermal resources for power generation

Egbert Jolie[1], Samuel Scott[2,3], James Faulds[4], Isabelle Chambefort[5], Guðni Axelsson[6], Luis Carlos Gutiérrez-Negrín[7], Simona Regenspurg[1], Moritz Ziegler[1], Bridget Ayling[4], Alexander Richter[8] and Meseret Teklemariam Zemedkun[9]

Abstract | Threats posed by the climate crisis have created an urgent need for sustainable green energy. Geothermal resources have the potential to provide up to 150 GWe of sustainable energy by 2050. However, the key challenge in successfully locating and drilling geothermal wells is to understand how the heterogeneous structure of the subsurface controls the existence of exploitable fluid reservoirs. In this Review, we discuss how key geological factors contribute to the profitable utilization of intermediate-temperature to high-temperature geothermal resources for power generation. The main driver of geothermal activity is elevated crustal heat flow, which is focused in regions of active magmatism and/or crustal thinning. Permeable structures such as faults exercise a primary control on local fluid flow patterns, with most upflow zones residing in complex fault interaction zones. Major risks in geothermal resource assessment and operation include locating sufficient permeability for fluid extraction, in addition to declining reservoir pressure and the potential of induced seismicity. Advanced computational methods permit effective integration of multiple datasets and, thus, can reduce potential risks. Future innovations involve engineered geothermal systems as well as supercritical and offshore geothermal resources, which could greatly expand the global application of geothermal energy but require detailed knowledge of the respective geological conditions.

Conventional geothermal resources
Naturally occurring convective hydrothermal systems heated by magma and/or a high geothermal gradient, with sufficient fluid and permeability to be exploited by flash or binary power plants

Flash power plants
Common technology for power generation from a two-phase, high-temperature geothermal reservoir by a steam turbine, with the option of multiple flash stages (single, double or triple).

Exergy
Thermodynamic measure of the maximum available work output from a system. Specific exergy (or availability) is defined as $e = h - h0 - T(s - s0)$, where h is specific enthalpy, T is absolute temperature, s is specific entropy and the subscript 0 refers to the reference or dead state (often taken to be 1 atm, 10 °C).

Vapour
Defined as fluid with a density that is lower than the critical density of the fluid composition in question; for geothermal systems, this term is interchangeable with steam.

Binary power plants
Common technology for power generation from a liquid-dominated, intermediate-temperature to high-temperature geothermal reservoir using heat exchangers to evaporate a working fluid with lower boiling point compared with water.

Climate change has accelerated ambitious renewable energy programmes like the European Green Deal or the Sustainable Energy for All initiative (United Nations), which aim to develop a low-carbon, resource-efficient, climate-resilient and climate-neutral planet. Geothermal energy can play a notable role in the transition from fossil fuels because it is independent of both daily or seasonal weather variations and unpredictable fluctuations of international commodity prices[1]. Geothermal resources are already used as a reliable energy source for heat and/or electricity in 90 countries[2,3]. Worldwide, the current installed capacity for electricity generation and direct utilization of thermal energy is between 15.5 and 16.0 GWe (gigawatts electrical)[2,4] and 107.7 GWth (gigawatts thermal)[3], respectively, leading to a total annual energy production of approximately 95.1 GWh (gigawatt hours)[2] and 283.6 TWh (terawatt hours)[3], respectively.

Geothermal systems are the near-surface expression of the heat transfer from the core of the Earth towards the surface. The vast majority of the Earth's internal heat is stored in the deep subsurface (>5 km), where the energy is not presently extractable using contemporary drilling techniques[1]. However, during hydrothermal convection, hot water can flow up through naturally permeable rocks and structures at sufficient rates to permit sustainable extraction through geothermal wells[5].

Active geothermal surface manifestations, such as hot springs or fumaroles, are relatively easy to find and can give insight into the best places to explore *intermediate-temperature geothermal systems* to *high-temperature geothermal systems*. However, hidden geothermal systems (sometimes also termed blind systems) lack active surface manifestations, although they may comprise the bulk of the geothermal resource potential, for example, in regions such as the Basin and Range Province in North America[6]. Locating these hidden systems and vectoring into the best sites for drilling geothermal wells in any system (hidden or not) requires advanced integration of geological, geophysical and geochemical features indicative of geothermal activity[7–10].

The characteristics of productive geothermal wells reflect a dynamic interplay between three major factors, including: heat source(s) and heat flow in the crust; permeability of faults, fracture networks and geological formations; and fluid flow patterns (such as large-scale groundwater convection, recharge and fluid chemistry)[11–13]. The geological controls range across scales from local prospects (such as permeable fracture networks and rock properties) to the regional volcanic and/or tectonic setting. Owing to all these complex and interrelated factors, the performance of geothermal wells can vary dramatically, both between different geothermal systems and/or within any given geothermal field or individual reservoir (even over short distances of tens to hundreds of metres)[14]. Geothermal exploration and targeting the best sites for drilling depends on understanding how various geological features interact to control fluid flow and resource characteristics.

Economically viable intermediate-temperature to high-temperature geothermal systems, used for power generation, only evolve where there is a combination of high heat flow and high permeability to allow fluid convection. Magmatism is the most efficient way to transfer heat into the shallow crust and, for this reason, most of the high-temperature prospects and production areas are located in volcanic provinces[15] (Fig. 1).

author addresses

[1] GFZ German research Centre for Geosciences, Potsdam, Germany.
[2] Iceland school of energy, Reykjavík university, Reykjavík, Iceland.
[3] institute of earth sciences, university of Iceland, Reykjavík, Iceland.
[4] Great Basin Center for Geothermal Energy, Nevada Bureau of Mines and Geology, University of Nevada, Reno, Nv, USA.
[5] Wairakei research Centre, GNs science, Taupō, New Zealand.
[6] GRÓ Geothermal training Programme, Reykjavík, Iceland.
[7] Geocónsul, Morelia, México.
[8] ThinkGeoEnergy, Reykjavík, Iceland.
[9] UNEP Africa Office, Nairobi, Kenya.

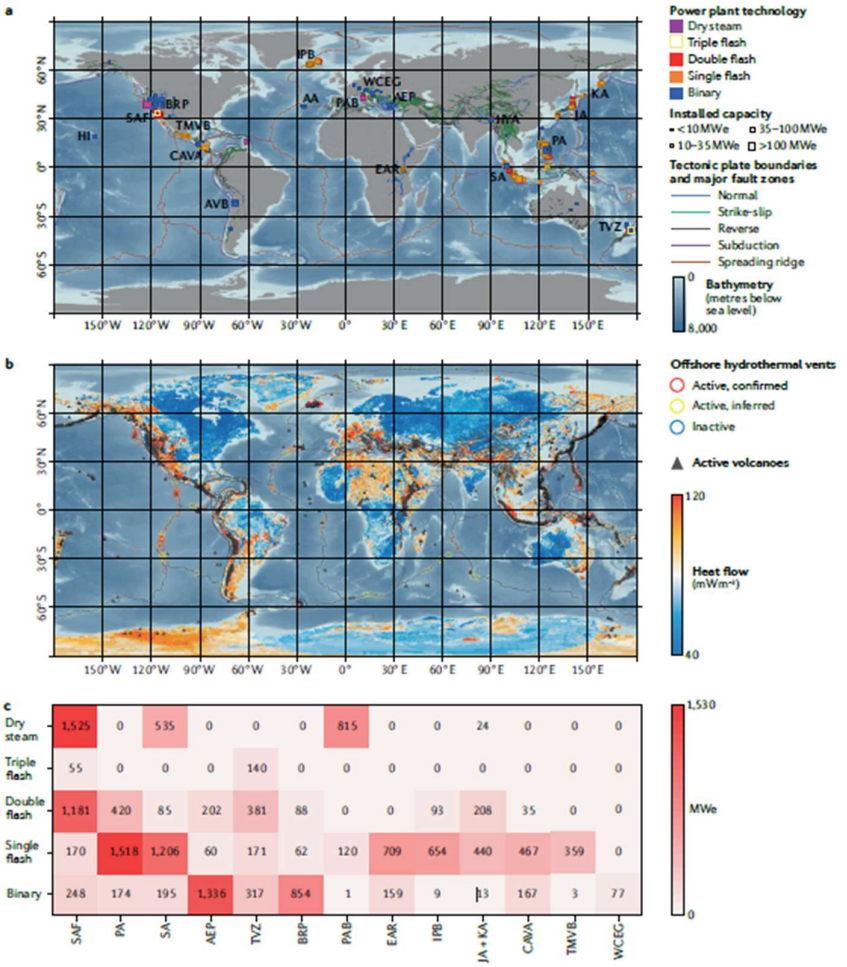

Figure 1. ***Global distribution of geothermal resources.*** *Exploitable intermediate-temperature to high-temperature geothermal reservoirs are mostly located near active volcanic areas and/or regions of crustal thinning.* ***a*** *| Key geothermal provinces with existing geothermal power plants relative to major fault zones and tectonic boundaries. Each geothermal province is characterized by a dominating power plant technology (binary, flash or dry steam power plants).* ***b*** *| Volcano-tectonic interaction, including tectonic plate boundaries, major fault zones, continental heat flow, offshore hydrothermal vent fields and active volcanoes.* ***c*** *| Total installed capacity for power generation (megawatts electric, MWe) is shown for each power plant technology from each of the key geothermal provinces shown in panel* ***a****. AA, Azores archipelago; AEP, Aegean extensional province; AVB, Andean Volcanic Belt; BRP, Basin and Range Province; CAVA, Central American Volcanic Arc; EAR, East African Rift; HI, Hawaii archipelago; HYA, Himalaya; IPB, Iceland plate boundary; JA, Japanese arc system; KA, Kuril arc; PA, Philippine arc; PAB, pre-Apennine belt; SA, Sunda arc; SAF, San Andreas Fault Zone; TMVB, Trans-Mexican Volcanic Belt; TVZ, Taupo Volcanic Zone; WCEG, western/ central European geothermal systems. Data from refs*[23,194–197].

Conventional geothermal resources are high-temperature systems (225 °C at less than 2 km depth)[16] with sufficient fluids and permeability to be exploited for power generation using conventional *flash power plants*. Alternative definitions of conventional resources can be based on other important geothermal resource factors, such as enthalpy, exergy or reservoir vapour fraction[17–19]. It is important to note, however, that even geothermal systems with intermediate temperatures of 125–225 °C are commonly capable of producing electricity using *binary power plants*, given favourable permeability conditions and sufficient fluid flow[20–22].

In continental crust outside areas of active magmatism, heat flow is generally lower (average ~67 mW m^{-2}; ref.[23]), meaning that conduction rather than convection dominates overall heat transfer. In these amagmatic regions, temperatures above 225 °C are typically only found at depths >4–5 km (ref.[24]), making extraction via conventional methods unfeasible where there is a lack of permeable structures and fluids. *Unconventional geothermal resources*, such as *petrothermal systems*, refer to geothermal resources in rocks with low porosity and permeability, where the lack of natural fluid flow means that artificial reservoirs need to be created and *enhanced geothermal system (EGS)* technology is required for extracting the energy at depth[25,26,27]. Application of EGS methods has been demonstrated in geothermal projects such as Soultz-sous-Forêts[28] or Fenton Hill[29].

In addition to temperature and permeability, the pressure and bulk fluid specific enthalpy of subsurface fluids are important controls on the power-producing potential of a geothermal resource. Several studies have indicated growing interest in geothermal systems with fluids at supercritical conditions in expectation of up to ten times higher well productivities[30,31]. In magmatic systems, tapping into supercritical geothermal resources for power production will require drilling closer to the heat source, where extreme corrosion, scaling and thermal stress challenges are found and have, thus far, acted as an inhibiting barrier to utilization of this resource[31,32]. Therefore, pursuing this opportunity will require innovations in drilling and well or surface materials needed for utilization.

In this Review, we provide an overview of how geological features influence the utilization of intermediate-temperature to high-temperature geothermal systems, with particular emphasis on the siting and effectiveness of geothermal wells. We describe how factors including heat flux, permeability structure and fluid properties control the productivity of geothermal wells. In addition, we consider how advances in computational methods, such as *geothermal play fairway analysis (PFA)*, machine learning (ML) and value of information (VOI) analysis are critical for the integration of multiple interdisciplinary datasets, reduction in the risks of geothermal exploration and, ultimately, for expansion of the future resource base.

Geological controls in geothermal systems

On a global scale, geothermal activity is focused in regions of relatively high heat flow resulting from active widespread magmatism and/or crustal thinning[33] (Fig. 1). This observation is also reflected in the global distribution of geothermal power plants.

Depending on the geological setting and characteristics of reservoir fluids, different power plant technologies are dominant in certain geothermal provinces (Fig. 1c). In this section, the geological settings, formations and structures that commonly host exploitable geothermal resources are reviewed.

Geological settings. The most productive geothermal wells are observed in Tertiary and older volcanic or volcaniclastic systems with well-developed, permeable fracture networks, rather than in younger volcanic or volcaniclastic systems[15]. The average geothermal gradient in the shallow continental crust (<5 km) is on the order of 25–30 °C km^{-1} (refs[24,34]) and typically relates to conductive heat transfer[35]. Geothermal gradients can be much higher in tectonically and/or volcanically active geothermal regions, where heat transfer is controlled by convection[15,33] (Fig. 2). Favourable tectonic settings include magmatic arcs (such as the Andean Volcanic Belt, Sunda arc in Indonesia, Philippine arc, Taupo Volcanic Zone or Japanese arc system), hotspots (including Yellowstone and Hawaii), transtensional pull-apart basins (for example, Salton Trough, Gulf of California) and both magmatic and amagmatic rifts (such as Iceland, the East African Rift, Basin and Range Province and mid-ocean ridges more generally)[33] (Fig. 1a,b).

Particularly prolific geothermal settings, such as Iceland or the Taupo Volcanic Zone, commonly correspond to regions experiencing both magmatism and crustal extension[36,37] (Fig. 1b), and are characterized by heat flow up to 600–800 mW m^{-2} in active geothermal areas[38,39]. However, amagmatic extensional settings also host large geothermal provinces, such as the Basin and Range Province of western North America (85 ± 10 mW m^{-2})[6,40] and the Aegean extensional province of western Turkey[41]. Regionally extensive, intermediate to high heat flow[24] characterizes such regions and extends well beyond individual volcanic centres in magmatic settings (Fig. 1b).

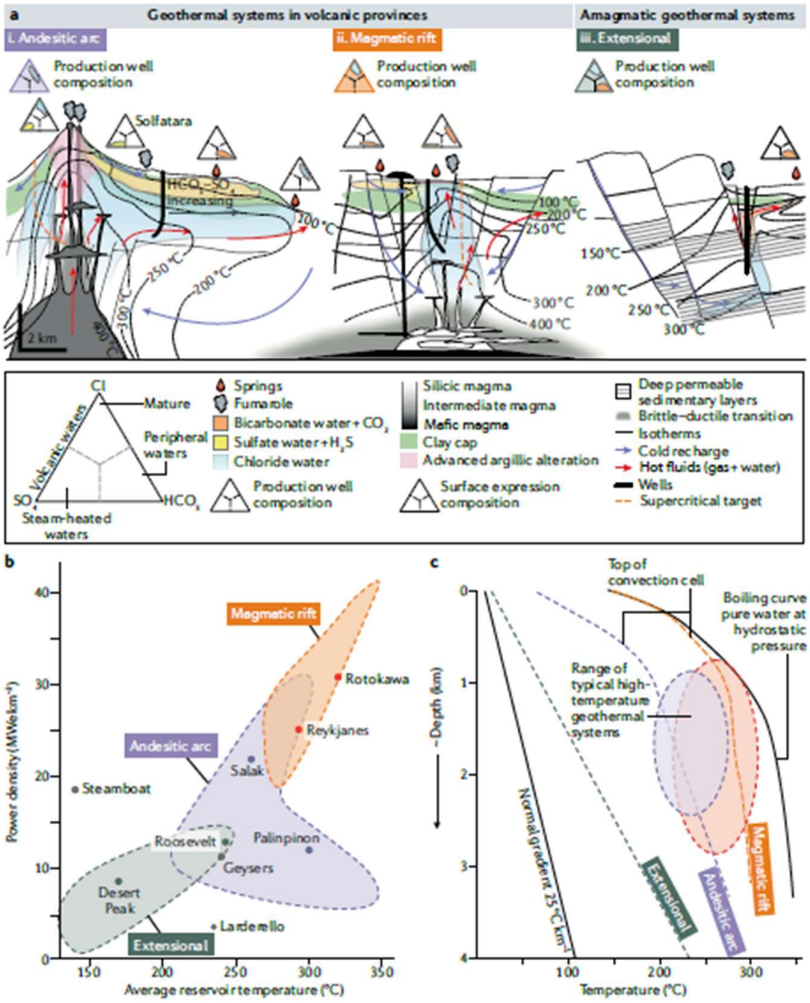

Figure 2. ***Typical geological settings of intermediate-temperature to high-temperature geothermal systems.*** *The optimal locations for geothermal wells are upflow zones located along permeable structures.* ***a*** *| Conceptual models of high-temperature geothermal systems with characteristic fluid chemistry in magmatic and non-magmatic environments. In volcanic andesitic arcs (i), the emplacement of intrusion(s) drives convection of surrounding groundwater. The high topographic relief of arc volcanoes results in lateral transport (outflow) of hot fluid. Magmatic degassing at the apex of the shallow magmatic intrusion generates acid-sulfate alteration associated with acid fluids. In magmatic rift environments (ii), active magmatism occurs at depth because of shallow mantle decompression. The extensional setting, accommodated by numerous normal faults, enhances the deep penetration of groundwater into the crust. In amagmatic extensional environments (iii), continental-scale extension leads to the thinning of the crust and elevated heat fluxes. Extensional faulting enhances groundwater downflow along permeable faults. The fluid is heated at depth and can travel laterally through permeable lithologies, before rising towards the surface along structural discontinuities. Production wells are placed in favourable structural settings, such as fault intersections or relay ramps.* ***b*** *| Power density (net MWe (megawatts electric) generated per km2 of surface footprint) versus average reservoir temperature[198,199].* ***c*** *| Temperature–depth profiles of different volcano-tectonic regimes15,200,201. Panel* ***a*** *adapted with permission from ref.[15], Elsevier. Panel* ***b*** *adapted with permission from ref.198, International Geothermal Association. Panel* ***c*** *adapted with permission from ref.[15], Elsevier.*

Three types of geothermal systems are observed in volcanic domains: andesitic arc systems (such as Awibengkok, Indonesia), silicic volcanic systems (Taupo Volcanic Zone, New Zealand, and Kyushu volcanic arc, Japan) and mafic systems (like the Iceland hotspot and East African Rift)[13,33,36]. Mafic systems can occur in continental settings or oceanic spreading centres, with a potential contribution from mantle plumes in some cases[15,33,36]. Optimal conditions for high-temperature geothermal systems develop in places where shallow magmatism occurs (Fig. 2a).

On a global scale, geothermal electricity is predominantly generated from volcanic arc systems[42]. Silicic volcanic systems, largely hosted by calderas and rhyolitic dome fields, are characterized by lower topographic relief relative to the andesitic volcanic

Unconventional geothermal resources
Geothermal systems (for example, petrothermal or supercritical resources) with potential for direct use or power generation, but demand specific enhancement and/or engineering of reservoir properties to become economically exploitable.

Petrothermal systems
Intermediate-temperature to high-temperature geological formations with low permeability (<10^{-16} m^2) and no fluid or insufficient fluid quantity.

Enhanced geothermal system
(EGS). Geothermal resource that is enhanced and/or artificially created (engineered) through hydraulic, chemical or thermal stimulation.

Supercritical geothermal resources
Potentially exploitable part of a high temperature geothermal system where permeability is $>10^{-16}$ m^2, and the temperature and specific enthalpy of water are greater than their critical values for pure water (374 °C, 2 MJ kg^{-1}).

Play fairway analysis (PFA)
Integrative approach to evaluate geothermal favorability, identify potential locations of blind geothermal systems and target the most promising sites for drilling geothermal wells.

Upflow zones
Areas where the hottest geothermal fluids flow upwards towards the surface along structural discontinuities and/or permeable formations.

Outflow zones
Areas where hot geothermal fluids flow laterally, commonly influenced by topography and faulting, normally at shallow depths (<1 km).

systems, which has a strong impact on the hydrogeological system (for example, location of upflow zones and outflow zones; Fig. 2a). Fluid circulation in the silicic systems is enhanced by the favourable permeability of silicic volcaniclastic rocks (≥10−15 m^2), as well as extensional or transtensional processes leading to fracturing, and high heat flow from underlying (>5 km) magmatic reservoirs or magma mush zones[33,43]. Oceanic spreading systems are mainly hosted by basaltic rocks, which are characterized by lower formation-hosted permeability but a denser fracture network[36].

Geological formations. Geothermal reservoirs can be hosted in multiple rock types, depending on the geological setting[13]. In active volcanic-type geothermal systems, reservoir lithologies are typically igneous rocks, including rhyolite, andesite, basalt and plutons; however, they can also include metamorphosed basement rocks[33]. In continental settings and amagmatic rifts, reservoir lithologies can include carbonates, metamorphic rocks (such as karstic marble, quartzite and schist), volcanic rocks (including basalt and basaltic andesite), plutons and sedimentary rocks (including volcaniclastics)[44–47].

The petrophysical properties of these geothermal reservoir rock formations and the subsurface temperature distribution play an important role in determining the location and volumes of geothermal fluid flow in the subsurface and, ultimately, well productivity and field energy output[5,48,49]. Porosity and permeability are two important characteristics that vary as a function of lithology, depth, stress regime and degree of hydrothermal alteration[50]. Both porosity and permeability typically decrease with depth, owing to burial and compaction-related processes[50]. However, some rock types are more likely to retain moderate to high primary porosity (up to ~30 vol.% for sandstone; ~70 vol.% for pumice) and primary permeability (10^{-14} to 10^{-16} m^2), such as some volcanic breccias, lava flows and pyroclastic flow deposits, and sedimentary rocks, such as sandstone or limestone (Fig. 3; ref.[50]).

Volcanic edifices can exhibit a wide range in primary permeability from ~10^{-19} to 10^{-11} m^2 (refs[51,52]). Secondary permeability plays an important role in many geothermal systems[53–55] and includes permeability associated with fractures and faults or rock dissolution (for example, in karstic carbonate formations) (Fig. 3). Secondary permeability occurs in almost all rock types (including metamorphic rocks, carbonates and igneous intrusions), and its presence means that even reservoir formations with low primary or matrix permeability (less than 10^{-17} m^2) can support productive geothermal systems[54,56].

In areas with elevated temperatures, the presence of sufficient permeability facilitates a complex series of feedbacks in reservoir formations. Where geothermal fluids circulate in the subsurface, water–rock interaction and hydrothermal alteration results in the dissolution of primary minerals and infilling of fractures and void spaces with secondary minerals[57]. These processes can increase or decrease porosity and permeability, and change the petrophysical properties of geothermal formations, such as density, sonic velocity and strength[52,58]. The intensity and type of alteration depends on the temperature, fluid chemistry, primary rock composition, permeability and duration of activity[57].

Alteration is typically characterized by the replacement of primary matrix minerals and by clay minerals (illite, smectite and kaolinite), zeolites and chlorite, with some adularia, quartz, calcite and epidote. The formation of clays, particularly swelling clays, causes a decrease in matrix porosity and permeability that can create an impermeable cap above intermediate-temperature to high-temperature resources[57,59]. Fractures and void spaces can also lose porosity and permeability, owing to precipitation of these secondary alteration minerals[52,54,56,60]. However, in some cases, fracture-filling mineral sequences show evidence of repeated sealing and refracturing because of imposed tectonic stresses, which serves to maintain effective permeability[53,61].

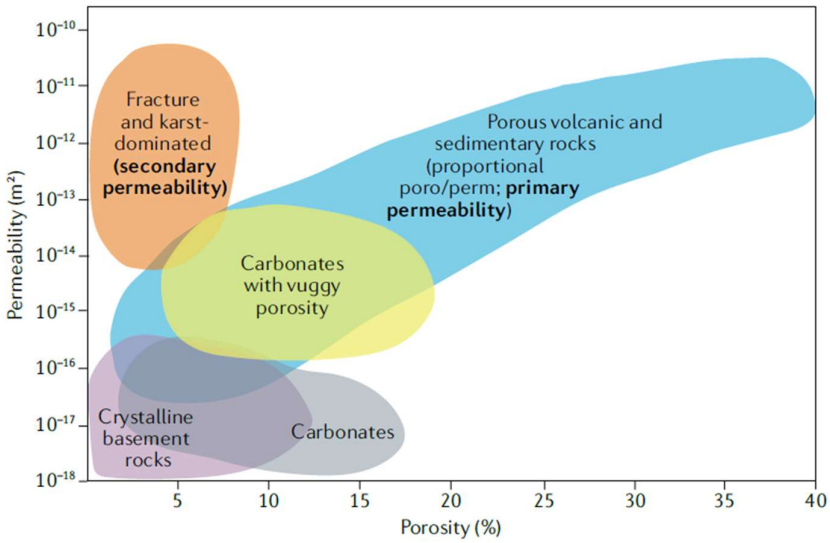

Figure 3. ***Porosity–permeability relationships in geothermal reservoir formations.*** *Conventional geothermal resources are typically hosted in reservoir formations that have permeabilities greater than 10−15 m^2. Unconventional geothermal resources have lower permeability. Adapted with permission from ref.[13], Elsevier, and modified to include data from refs[51,139,202,203].*

Permeable structures. Structures (fractures and faults) play a key role in localizing permeability (commonly referred to as secondary permeability) in intermediate-temperature to high-temperature convective geothermal systems, as indicated by the

Liquid-dominated geothermal resource
Able to produce a mixture of liquid and vapour (steam), and generally the most common resource type.

Vapour-dominated geothermal resource
Able to produce only vapour (steam), generally a less common resource than liquid-dominated systems.

correspondence of well feed-zone locations with highly fractured intervals[62]. Formation-mediated fracture permeability is generated as a result of local-scale to regional-scale tectonic stresses and, thus, can be formed in any lithology that has sufficient strength and mechanical competence to host fractures[63].

At the most fundamental level, faults and fracture systems serve as channels for geothermal fluids[64–67] from hot deeper levels of the crust to within a few kilometers of the surface, where wells can tap the fluids for power production. Conversely, such structures also facilitate the circulation of meteoric fluids from near the surface to deeper crustal levels (termed recharge), which is essential for sustaining broad convective geothermal systems39. The primary challenge for commercial development and productive wells in those areas is locating fluid-bearing permeable structures with sustainable recharge at exploitable levels of the crust.

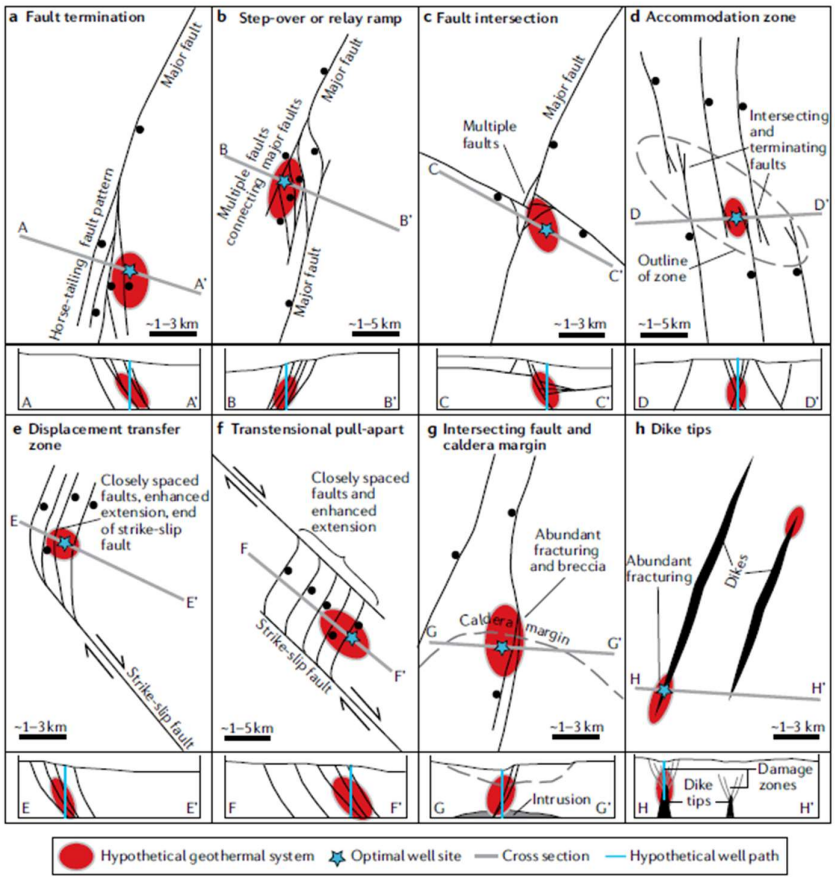

Figure 4. ***Favourable structural settings for geothermal exploitation.*** *Most common permeable structures are located in extensional or transtensional settings. Red shaded areas mark approximate locations of hypothetical geothermal upwellings in map view and in cross section. Blue stars and lines illustrate hypothetical optimal well sites and well paths, respectively. Double arrows indicate the orientation of the maximum horizontal stress.* ***a*** *|* *Fault tip showing horse-tailing pattern of closely spaced faults at the termination of a major normal fault.* ***b*** *|* *Step-over or breached relay ramp showing abundant minor faults connecting overlapping strands of a major normal fault zone.* ***c*** *|* *Fault intersection with abundant minor faults proximal to the intersection.* ***d*** *|* *Accommodation zone (marked by grey ellipse) encompassing a belt of terminating, overlapping and intersecting normal faults.* ***e*** *|* *Displacement transfer zone whereby a major strike-slip fault terminates in an array of normal faults.* ***f*** *|* *Transtensional pull-apart incorporating multiple closely spaced normal faults connecting a releasing step in a major strike-slip fault.* ***g*** *|* *Intersecting normal fault and caldera margin (thick dashed grey line).* ***h*** *|* *Dike tip or termination, whereby abundant fracturing characterizes the damage zone proximal to the tip of a dike. Adapted with permission from ref.6, International Geothermal Association.*

Most intermediate-temperature (≥125 °C) to high-temperature geothermal systems (≥225 °C) reside along normal faults in complex interaction zones, such as fault terminations, fault intersections, step-overs or relay ramps, accommodation zones, displacement transfer zones and releasing bends or pull-aparts[6,68] (Fig. 4). Terminations of major faults commonly consist of multiple closely spaced fault strands in horse-tailing splays (Fig. 4a). Relay ramps are typically breached by abundant minor faults connecting the larger overlapping fault strands (Fig. 4b,c; refs[69,70]). Accommodation zones consist of oppositely dipping intermeshing fault systems and, thus, consist of multiple fault terminations and intersecting faults (Fig. 4d; ref.[71]). Displacement transfer zones in transtensional settings are comprised of a series of normal faults at the termination of a major strike-slip fault (Fig. 4e,f; ref.[6]). Thus, these fault interaction zones contain higher fault and fracture densities, are characterized by more permeable fault breccia in lieu of impermeable clay gouge along main fault segments and typically correspond to critically stressed areas[6,8,72]. Enhanced fracture permeability, minimal stress relief by major earthquakes and lack of pervasive healing of faults and fractures facilitate long-term fluid flow in these fault interaction zones[73].

There are many examples of commercially viable geothermal systems residing in fault interaction zones, including the Brady and Desert Peak systems that occupy relay ramps in the Basin and Range Province of the USA74; Germancek and Kızıldere systems that occupy major fault terminations in the Menderes graben of western Turkey75; several major systems residing in broad accommodation zones, relay ramps or fault terminations in the Taupo Volcanic Zone of New Zealand[76]; and systems that occupy broad pull-aparts along strike-slip fault zones in Sumatra, Indonesia[77] and the Salton Trough in southern California, USA[78]. Most of these systems host operating geothermal power plants.

Complex structural settings with more than one type of favourable structure host robust geothermal systems[79]. For example, accommodation zones[71], which incorporate multiple fault terminations and intersections, host some of the most productive systems in the Basin and Range Province of the western USA (such as Steamboat and McGinness Hills[6]) and in the Taupo Volcanic Zone of New Zealand (including Ohaaki-Broadlands and Wairakei[76]). Reported values of effective reservoir permeability are

rare in the literature[50], but production flow rates of wells provide indications of favourable permeability. Geothermal production wells within fault interaction zones in the Basin and Range Province generally yield flow rates ranging from ~10 to >300 litres per second, with average rates commonly exceeding 100 litres per second in the more complex structural settings with more than one type of favourable structure[80].

Similar complex structural settings (such as fault intersection zones) also characterize most (nearly 75%) of the volcano-hosted geothermal systems[68], particularly in regions undergoing extension or transtension[81]. However, magmatic settings also generate additional types of permeable structures, including caldera margins, dike tips and intense zones of fracturing surrounding intrusions[36,67] (Fig. 4g,h). Notably, in areas with magmatic heat sources, abundant fractures coupled with relatively thick, permeable stratigraphic horizons can provide adequate hosts for large geothermal reservoirs in the absence of a fault interaction zone, as possibly exemplified by some systems — for example, Rotokawa in the Taupo Volcanic Zone[55].

Understanding the current stress field through regional stress field modelling, fault kinematic and/or borehole breakout data[82-86] is critical for defining which structures are most likely to channel fluids as faults and fractures oriented approximately orthogonal to the least principal stress in the regional stress field are most conducive to accommodating geothermal fluid flow[63,87] and can, ultimately, be targeted for geothermal drilling. Quantitative stress analyses also provide important information for modelling the risk of induced seismic events of potential economic and social concern[88,89]. Superimposed on the regional stress regime, lithological heterogeneities (such as formation boundaries, the edges of a pluton, caldera margins and dike intrusions) can serve to modify the local stress conditions and favour the development and dilatation of natural fractures serving as productive feed zones in geothermal systems[90].

Box 1 | ***Power generation potential***

The power output from a geothermal reservoir depends on the enthalpy of produced fluids, the mass flow rate from production wells and the efficiency at which the thermal energy of the fluid is converted to electricity. the enthalpy of well discharge fluids is often close to that of saturated liquid at 200–250 °C, but can also be notably higher, owing to phase segregation and boiling.

Thermodynamic availability[206] is defined as the maximum amount of electrical power that can be produced from reservoir fluids at a given pressure and temperature (see Box figure). availability increases with the vapour content of boiling fluids and temperature. The availability of water at 450 °C and 25 MPa is approximately six times that of 250 °C boiling water. Moreover, supercritical temperatures reduce fluid viscosity and increase compressibility, resulting in higher fluid mobility and mass flow rates in production wells. increasing pressure at supercritical temperatures decreases availability.

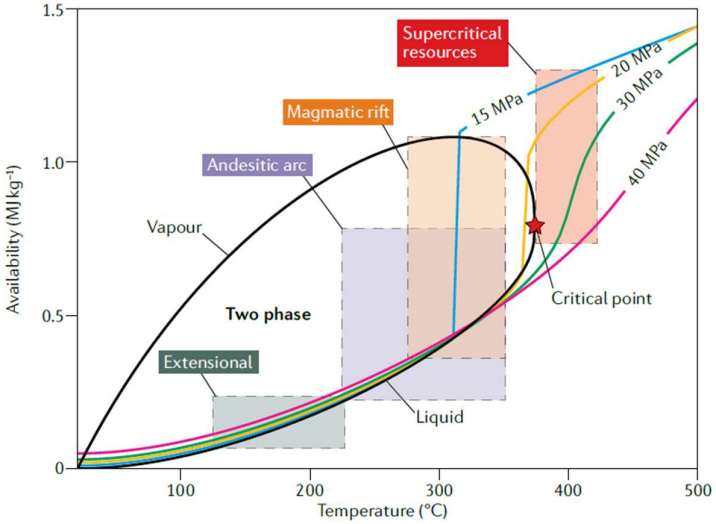

Fluids in geothermal systems

Geothermal fluids circulating in permeable rocks and fractures transport energy from the deep heat source to the surface, and consist of both vapour and liquid (brine) phases of variable composition. Fluids in geothermal systems of meteoric origin are commonly dilute, containing 1–5 wt.% total dissolved solids (TDS)[91], whereas certain systems contain highly saline reservoir fluids with up to 30 wt.% TDS (ref.[92]). Fluid chemical analyses constitute a key tool for assessing the production characteristics of geothermal wells, providing important information on fluid origin, circulation patterns, evolution, temperature and recharge[91]. However, the chemical characteristics of deep fluids are changed by boiling, mixing and cooling processes during ascent to the surface[93], which can make interpretation of the fluid chemistry more complicated. In this section, we discuss the general properties of deep fluids and processes they undergo within the hydrothermal system, and the effect of energetic fluid properties on operational conditions.

General fluid properties and processes. High-temperature fluids in geothermal systems dominantly result from the circulation of meteoric fluids to the depth of the heat source[94], where they are heated and ascend because of the decreased fluid density. The size of the surface and subsurface catchment area depends largely on the structural and geological characteristics[95]. Major fault zones can channel fluids to and from geothermal resources over long distances[96,97]. Meteoric fluids can also mix with substantial amounts of seawater, magmatic volatiles or connate fluids[59,91,98,99]. Primary geothermal fluids in the base of upflow zones ascend during density-driven convection and undergo processes such as fluid–rock interaction, depressurization, boiling, cooling, condensation, phase segregation and variable mixing[93]. Dissolution of primary host rock minerals by the hot, volatile-rich fluid enriches the fluids with chloride and other incompatible elements (B, F), particularly if the fluids have interacted with evaporitic sedimentary rocks[59,92]. The formation of alteration minerals such as quartz (SiO_2), Ca–Al silicates, calcite ($CaCO_3$) and pyrite (FeS_2) controls the temperature-dependent concentrations of non-volatile components (Si, Na, K, Ca, Fe, Mg), volatiles (CO_2, H_2S, H_2) and solution pH (ref.[100]). In addition to host rock dissolution, magmatic or mantle degassing is a major source of volatiles in geothermal fluids[64,101,102].

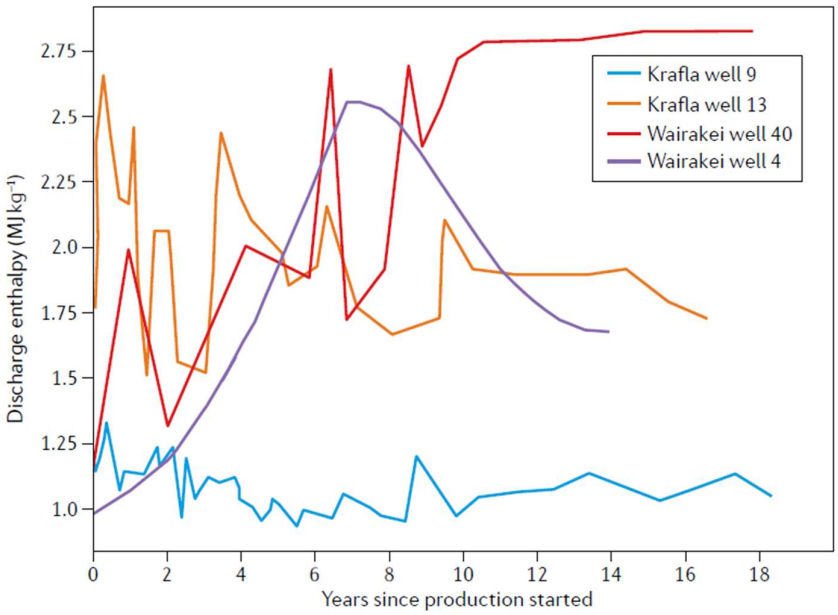

Figure 5. ***Evolution of discharge enthalpy in geothermal wells.*** *Many wells that tap liquid-dominated reservoir fluids show nearly constant discharge enthalpy (Krafla well 9). The discharge enthalpy of wells that tap boiling reservoirs can be much higher and show greater fluctuations (Krafla well 13). Fluid withdrawal and pressure decrease can also induce boiling in the reservoir, as indicated by wells with a discharge enthalpy initially close to liquid enthalpy that increases with time to dry steam (Wairakei well 40). However, this increase might also be followed by a decrease in enthalpy, potentially indicating cold water recharge into the reservoir (Wairakei well 4). Data from refs*[116,117].

Liquid–vapour coexistence is widespread in the upflow zones of high-temperature geothermal systems[93]. For pure water, liquid–vapour coexistence can occur at temperatures and pressures below the critical point of pure water (374 °C, 221 bar)[103]. However, natural geothermal fluids are multicomponent fluids, for which liquid–vapour coexistence can extend to much greater temperatures and pressures[104]. Boiling leads to the enrichment of non-volatiles in the liquid phase and the exchange of volatiles between the liquid and the vapour phases[93]. In contrast, the condensation of liquid from vapour leads to the transfer of volatile components to the liquid phase[93].

Whether a system is a liquid-dominated geothermal resource or a vapour-dominated geothermal resource or shows hybrid characteristics depends on the geological controls, including the energy of the heat source, the permeability structure, as well as large-scale groundwater convection patterns[11,12,105–107]. Most geothermal reservoirs consist of sub-boiling liquid or boiling liquid with a small fraction of vapour by mass (0–5%; ref.[93]). Geothermal wells in vapour-dominated geothermal systems, like The Geysers (USA), Kamojang (Indonesia) or Larderello (Italy), discharge single-phase saturated or superheated vapour, but produce from reservoirs that can contain an immobile liquid phase trapped in a tight matrix rock[108]. Many liquid-dominated geothermal systems develop shallow vapour-rich boiling zones109, which can be attractive for geothermal power generation, owing to high well enthalpy and relative ease of targeting.

Boiling leads to phase segregation, owing to contrasting buoyancy, viscosity and relative permeability, and ascent of H_2S-bearing or CO_2-bearing vapour. Condensation of liquid from the ascending vapour by heat loss or mixing with surface water results in the formation of acid sulfate-rich and bicarbonate-rich waters[93]. The acidic waters effectively dissolve the primary minerals of common volcanic rocks, leaving a residue rich in amorphous silica and smectite, among other minerals[110]. The alteration of rocks to smectite-rich assemblages reduces rock strength and fracture cohesion[58], inhibiting the formation of high-permeability extensional fractures[60]. The formation of low-permeability caps can enhance the productive capacity of the reservoir by preventing cooling of geothermal reservoirs by surface water influx and expands the prospective resource area by directing outflow of buoyant water laterally updip along the base of the clay cap[48]. Smectite becomes unstable at temperatures >200 °C (ref.[111]) and, as temperature increases further, alteration minerals such as chlorite, epidote and actinolite become increasingly pervasive[57,112].

Relevance of fluid properties. The enthalpy of geothermal fluids exerts a major control on the power-producing potential of a geothermal reservoir (Box 1). The much higher power generation potential of vapour-dominated geothermal systems is mainly a consequence of the much higher enthalpy of vapour compared with that of hot liquid. Many wells drilled into liquid-dominated geothermal reservoirs discharge fluid with an enthalpy close to that of single-phase liquid at the aquifer temperature (1–1.5 MJ kg^{-1}); however, it is not uncommon for certain wells to develop discharge enthalpies as high as 2.7 MJ kg^{-1}, corresponding to the specific enthalpy of saturated vapour[93]. These high discharge enthalpies could indicate a substantial vapour fraction in the aquifer fluid[113,114] or the presence of multiple feed zones (for example, a shallow vapour-dominated feed zone and a deep liquid feed zone), although high well discharge enthalpy can also result from boiling and phase segregation in the zone of depressurization surrounding wells[93,114,115]. In addition, marked changes in well discharge enthalpy are observed over time, resulting from increased boiling or cooling of the reservoir by cold water recharge[116,117] (Fig. 5).

The chemical composition of geothermal fluids can pose a major operational risk of scaling (precipitation of solid phases such as amorphous silica, calcite and Fe–Mg sulfides), which result from changes in the pressure–temperature conditions or degassing of liquid with a high TDS content[118–120]. In addition, solute-rich geothermal fluids have a higher acidity and are more aggressive, which can lead to corrosion of the well casing or surface equipment[120]. In order to mitigate the risk of corrosion or scaling, most geothermal wells target alkali-chloride waters (dilute waters with near-neutral pH and Si, Na and Cl as dominant components in the liquid phase) at depths 1–3 km and temperatures of 200–350 °C (Fig. 2; ref.[59]). Phase separation at high temperatures (>350 °C) in the proximity of the heat source can give rise to high-salinity brines121, which also pose an increased risk for corrosion and scaling[118].

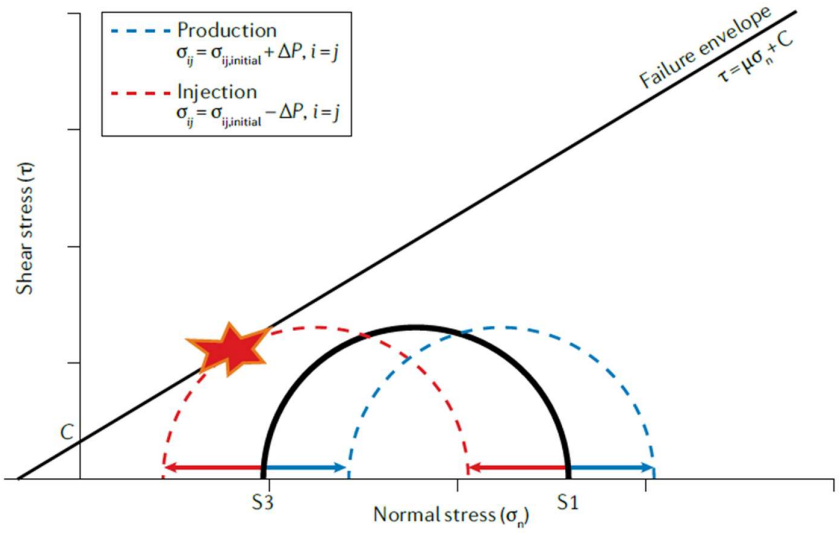

Figure 6. ***Failure criterion for a critically stressed fault.*** *Mohr–Coulomb diagram with the normal stress (σn), shear stress (τ) and a failure criterion (black line) defined by τ = μ * σn + C, with the friction coefficient μ and the cohesion C (ref.[204]). If the Mohr circle defined by the magnitudes of the maximum (S1) and minimum (S3) principal stress components touches the failure envelope, the rock fails. In some circumstances, this can lead to induced seismic events of economic concern. Any change in the pore pressure (ΔP) affects the stress tensor (σij) in its normal components where i = j. Fluid injection destabilizes the stress state (moves closer to failure envelope) and production stabilizes the stress state (moves away from failure envelope)[205].*

Sulfate-rich waters formed at depth by disproportionation of HCl and SO_2 that has degassed from a magmatic heat source[122,123] or acid-sulfate waters formed near the surface by oxidation of H_2S (ref.[93]) are generally unsuitable for power generation because of their high acidity (pH < 4). Wells with higher discharge enthalpy produce less liquid at the surface, mitigating the risks of scaling. For the sustainable management of a reservoir, it is important that all liquid produced from geothermal wells is reinjected, which is also important for the disposal of geothermal fluids[124]. This requirement poses a major operational challenge, because mineral precipitation owing to boiling or cooling in the near proximity of a production or reinjection well[125] can result in decreasing rates of fluid extraction or fluid injectivity with time[126,127].

Geothermal wells

Wells are the conduits to bring geothermal fluids to the surface and, during the exploration stage of a new field, are the ultimate way to prove the existence of a geothermal reservoir. The optimal location and construction of geothermal wells is fundamental for a successful geothermal development. The success in selecting the location of a geothermal well depends on a comprehensive understanding of the structural and stratigraphic controls on subsurface geothermal reservoirs. In this section, we discuss the different types of wells, their variable capacity, associated risks, as well as new drilling concepts.

Main features of geothermal wells. Geothermal wells can be classified based on their primary purpose, which can be either investigation (thermal gradient, exploration) or resource utilization (production, reinjection or monitoring). Thermal gradient wells are a special type of exploratory well, typically drilled to relatively shallow depths (50–200 m), with the primary goal of estimating heat flow. These wells are especially useful in the exploration of fracture-controlled intermediate-temperature resources or EGSs. Exploratory wells can be either slim wells with relatively small diameter (<6 inches or <15.2 cm) to assess conditions at reservoir depth or larger diameter wells that can be used as production wells if successful1[28]. Production wells discharge single-phase vapour, single-phase liquid or a two-phase mixture, and are designed to naturally discharge but, in some cases, the discharge is aided by downhole pumps[129]. Reinjection wells are used to return the residual brine to replenish the geothermal reservoir, avoid possible contamination of shallow aquifers and to inject water of a different origin if needed as supplemental recharge, with the objective of compensating declining reservoir pressure owing to utilization[124]. In any case, reinjection must be appropriately managed to avoid premature cooling[130]. Both production and reinjection wells can be used as make-up wells to mitigate declining well capacity or failure. Monitoring wells are mainly used to assess changes in pressure and temperature in the geothermal reservoir, collect data to improve the conceptual model of the geothermal system and plan the location of new wells, and constrain numerical reservoir models[131].

Drilling geothermal wells is broadly comparable to drilling oil and gas wells, with a drill bit penetrating subsurface rock, although there are some fundamental differences (such as larger well diameter for geothermal production wells). The resulting rock cuttings are transported to the surface by a drilling medium, which can be water, drilling mud, compressed air or aerated liquids[128]. Extracting rock core from drill holes provides more complete information on the composition and mechanical properties of potential reservoir rocks, but are less commonly drilled because of their greater expense. Geothermal wells can either be vertical or directional (deviated), usually with the angle from the vertical less than 45°. A few (typically around one to four) metallic pipe casings, telescopic in structure, are cemented in the shallow part of the well, above the production interval. Below the casing, the production or reinjection part of the well can be left open (uncased) or have a slotted liner casing hung from the bottom of the cemented casing. The precise placement of the production casing along the drill string is defined by the key geological controls, in particular, the location of permeable fracture zones (feed zones).

The thermal power of geothermal wells drilled into intermediate-temperature to high-temperature geothermal resources ranges from 1 to 100 MWth (megawatts thermal)[20]. At realistic thermal efficiencies of 10–20% (ref.[132]), geothermal wells generate 3–5 MWe (megawatts electrical) per well on average worldwide[133]. However, especially productive wells can generate between 10 and 50 MWe, particularly during the early stages of exploitation[20,134]. The largest geothermal field used for power generation is The Geysers in the USA, with an installed capacity of 1.6 GWe and current power generation between 750 and 800 MWe (ref.[135]). The current installed capacity worldwide is between 15.5 and 16.0 GWe (refs[2,4]), but the increased utilization of

conventional, geothermal resources and a wider development of EGSs could increase the total installed capacity to 150 GWe by 2050 (refs[1,136]).

Drilling risks and challenges. There are considerable risks associated with drilling geothermal wells, and their ultimate capacity is often difficult to estimate. Analysis of more than 2,600 geothermal wells worldwide[134] showed a success rate (defined by a capacity of ≥3 MWe per well) of at least 78%, which increases with the number of wells drilled in a particular field. Notably, permeability can vary substantially on the scale of tens to hundreds of metres, owing to the inherent variability in the characteristics of permeable structures and rock units. Thus, successful wells that have penetrated permeable structures or rock units can be located proximal to unsuccessful wells drilled into relatively impermeable zones[14].

Faults can also act as hydraulic barriers, which results in compartmentalized geothermal reservoirs[55]. It is, therefore, imperative that the geological, geophysical and geochemical features indicative of geothermal activity are fully understood in a particular area prior to drilling. In addition, for suboptimal wells that have not intersected sufficiently permeable structures, hydraulic stimulation can improve near-well permeability and open hydraulic connections to nearby permeable zones[137]. For this purpose, concepts like cyclic soft stimulation[138] can be applied for the controlled injection of water at increased pressures. Chemical stimulation is another approach to improving reservoir permeability, whereby additives are used to dissolve material filling fractures or pore space (such as calcite). The intermittent reinjection of cold water can also lead to thermal shocking and further thermal stimulation[137,139,140].

In all systems, faults and fractures oriented approximately orthogonal to the least principal stress in the current stress field are most conducive to accommodating geothermal fluid flow[63,87]. If the current stress state is known, slip and dilation tendency analyses[141,142] can be carried out to provide a quantitative indication of the likelihood of certain fault segments to be critically stressed and, therefore, conduct fluids. Coincidentally, elevated fault criticality indicates a potential for induced seismicity due to the pore pressure changes associated with geothermal utilization (extraction and reinjection of fluids), which can be visualized by a Mohr–Coulomb diagram[88,89,143] (Fig. 6). Reinjection and stimulation induce seismicity under particular geological conditions[89,143]; however, the economic risk associated with induced seismicity can be reduced by appropriate mitigation strategies[142,144], such as aforementioned soft stimulation or stimulation operations controlled by a rigorous monitoring of seismicity[145].

Other risks associated with geothermal wells are related to the impact of drilling on the reservoir, as well as changes in well discharge properties following long-term utilization of a geothermal system (Fig. 5). For example, near-well permeability can be impaired owing to drilling mud and/or drill cuttings[129]. Risks associated with the operation of geothermal wells include casing collapses because of deficient cementing and/or thermal stresses, potentially requiring workovers and/or side-tracking of more severely damaged portions of the well[128].

Scaling and corrosion constitute additional risks for geothermal wells[118–120]. Precipitation of amorphous silica is the most common scaling risk in high-temperature systems146, although carbonate, iron-magnesium, iron-silicate, metal sulfide or sulfate scales can also form[125,146–148]. High temperatures, low pH, high salinities and gases induce different types of corrosion at many geothermal plants[120], including: general, pitting, crevice and galvanic corrosion; sulfide stress corrosion cracking; or hydrogen embrittlement. In many cases, scaling and corrosion can be mitigated through the use of chemical inhibitors[149], rapid cooling, ageing and mixing with steam[126,146,150,151], as well as control of the reinjection temperature[146].

The primary risk associated with the long-term utilization of geothermal reservoirs is declining reservoir pressure, which generally causes well output to decline[129,131]. In liquid-dominated wells equipped with downhole pumps, production is limited by a maximum allowable pressure drawdown. In two-phase wells that discharge spontaneously through boiling, declining reservoir pressure can, in some cases, stimulate boiling, increasing well discharge enthalpy and energy output[116,117,129,131] (Fig. 5). Declining reservoir pressure can, furthermore, increase non-condensable gas content and/or lead to recharge of cooler liquid[116]. The risk of declining well output with time highlights the importance of monitoring the response of geothermal wells and reservoirs during long-term utilization[129,131]. Furthermore, these data can contribute to the sustainable use of geothermal resources, which is exemplified by systems that have been utilized for several decades, and demonstrate that a semi-balance between net energy discharge and recharge can be achieved by maintaining production below a certain limit[5].

New drilling concepts, including innovative materials and casings, are required for wells targeting the deeper roots of volcanic geothermal systems potentially containing supercritical fluids, which have yet to be utilized[152]. Good examples of wells targeting unconventional geothermal resources are the wells of the Iceland Deep Drilling Project (IDDP), which aim to drill down to 4–5 km depth in high-temperature volcanic systems. Well IDDP-1 encountered magma at about 2 km depth beneath the Krafla geothermal system and yielded the equivalent of ~35 MWe before collapsing because of extreme conditions[153]. Well IDDP-2 reached ~4.7 km depth beneath the Reykjanes geothermal system, where a temperature of 500–550 °C was inferred[154]. Although operational challenges rendered both of these wells unable to produce, the wells did demonstrate the presence of high permeability in the near-magma environment and in the deep, high-temperature roots of geothermal systems.

Summary and future perspectives

Intermediate-temperature to high-temperature geothermal systems can be found in a variety of volcano-tectonic settings, including magmatic arcs, hotspots, magmatic and amagmatic continental rifts, and transtensional pull-apart basins. Elevated heat flow, permeable structures and circulating fluids are the key ingredients for a commercially viable, conventional geothermal resource. The expression of these geological controls varies across scales ranging from the regional setting (heat flow, structural setting) to the local prospect (permeable lithological units and individual structures, physico-chemical properties of reservoir fluids).

Understanding the spatial distribution of these features in the subsurface presents key challenges, which are compounded by the likelihood that a large number of geothermal systems are hidden with no surface manifestations, such as hot springs or fumaroles. Thus, exploration of greenfield geothermal resource areas, selection of optimal sites for drilling geothermal wells and, ultimately, the long-term sustainable management of a geothermal resource for power generation all require a detailed understanding of the geological factors controlling the system. Here, we summarize the key advances in geothermal exploration to date and discuss our opinion of targets for future prospecting and technology.

Unconventional geothermal resources. Conventional geothermal resources have been successfully developed for power generation for more than 100 years[20]. Projects can build on decades of experience, proven and established exploration methods and technologies. However, further innovations are required to unlock an immense resource base at higher temperatures and greater depths, as well as unleash the vast untapped potential of EGSs. A multidisciplinary workflow, involving geological, geophysical and geochemical analyses, must be carried out to reduce the risks in geothermal development. Even in relatively well understood systems, new wells entail careful planning to ensure the presence of sufficient permeability, high enough fluid temperatures and adequate flow rates, as well as mitigating any effects of challenging fluid chemistry.

Unconventional geothermal resources are characterized by more extreme reservoir properties compared with conventional geothermal resources used for power generation. Owing to low in situ rock permeability, extremely high fluid temperatures, challenging fluid chemistry or offshore conditions, the wider development of unconventional resources will require novel advances in exploration and engineering technologies. Engineered geothermal systems, in which permeability is artificially enhanced through hydraulic, chemical or thermal stimulation, hold promise for substantially expanding geothermal resources in the future. Commonly, rock units have existing natural fracture networks, which can be stimulated and reactivated. To date, EGS experiments and demonstration projects[25] have been conducted in mechanically competent, crystalline basement lithologies that are amenable to stimulation, including plutonic rocks (granites, granodiorite), metamorphic rocks (gneiss, greywacke), metasedimentary rocks and metavolcanic rocks[25,26,27].

In addition, there is growing interest in expanding the geothermal resource base to include greater depths (>3 km) and higher temperatures (>350 °C). Accordingly, there are projects aimed at tapping into the deep roots of magma-driven geothermal systems in Iceland[153–155], Japan[156], the USA[157], Italy[31,158], Mexico[159] and New Zealand[160]. Fluids at temperatures and pressures greater than the critical point of pure water (374 °C, 221 bar) are often referred to as superheated or supercritical, depending on whether the fluid pressure also exceeds the critical pressure of pure water, respectively. However, such terminology is problematic, as all fluids in geothermal systems are multicomponent fluids, which show liquid–vapour coexistence extending to much higher temperatures and pressures[161]. In such fluids, critical behaviour occurs along critical curves and raising temperature above the critical temperature at a given pressure results in fluid phase separation, rather than homogenization[161]. The potential to drill wells that tap a high-enthalpy (>3 MJ kg^{-1}) intermediate-density vapour underlying conventional geothermal resources is attractive because of the exceptionally high rates of mass transport resulting from the much higher ratio of buoyancy to viscous forces and improved efficiency of power production at higher temperatures[30].

Owing to the growing interest in targeting supercritical geothermal resources, several studies have sought to understand vapour formation processes in the proximity of a magmatic heat source162–164. Measurements from the IDDP-1 discharge fluid suggest that the concentrations of volatile elements (B, C and S) were similar to the subcritical geothermal reservoir fluid, whereas the concentrations of mineral-forming elements (Si, Na, K, Ca, Mg and Cl) were much lower[165]. Thus, it was proposed that vapour formation results from near-isobaric conductive heating of conventional subcritical geothermal fluids and quartz-dominated mineral precipitation during boiling of liquid to dryness[162]. Numerical modelling of fluid circulation in permeable rocks (10^{-14} to 10^{-15} m^2) surrounding magmatic intrusions shows that the extent and temperature of supercritical geothermal resources depend on permeability, resource depth, fluid salinity and fluid–rock interaction[121,163,164,166]. The IDDP initially sought to drill to depths >4 km to tap into geothermal reservoirs with supercritical pressures; however, the high power-producing potential despite the shallower than expected drilled depth shows that economically attractive high-enthalpy vapour discharges can develop also at subcritical pressures in the proximity of intrusions.

Early conceptual models of the near-magma geothermal resource proposed a major permeability decrease at 350 °C, corresponding to a transition in the dominant mode of rock deformation from brittle fracture to ductile flow[167,168], although more experimental results have since shown how permeability gradually changes in response to the onset of plastic normal deformation of a fracture surface[169]. In basaltic rock in laboratory settings, brittle deformation is observed at temperatures >550 °C (refs[170,171]), in agreement with results from the IDDP-2 well, which revealed high permeability up to 4.5 km depth[154]. However, low permeability has been encountered in several deep geothermal wells[31,172], and novel permeability enhancement techniques in superhot geothermal resources have received substantial research attention[173–175]. Further, enabling the expansion of the geothermal resource base to include supercritical and near-magma geothermal resources will also require innovations in drilling techniques[152,176] and surface materials[32]. Despite these challenges, accessing these resources could improve the economics and sustainability of power generation from high-temperature geothermal systems in the future.

Promising resources could also be located offshore in hydrothermal vent fields along mid-ocean ridges (Fig. 1b), where elevated fluid pressures at the surface of the ocean floor induce development of hydrothermal systems with temperatures >380 °C at crustal depths of <1 km (ref.[177]). Other potential exploration areas have been identified in Iceland (such as offshore Reykjanes Ridge), Italy (Southern Tyrrhenian Sea) and Mexico (Gulf of California)[178–180].

The success of EGS projects depends not only on a deep understanding of the subsurface and wider adoption of innovative exploration concepts and exploitation technologies but it is also crucial to actively promote wider social acceptance of utilization

of geothermal resources among the general population. Social concerns have to be addressed from the very beginning. This requires professional, fact-based communication with all involved stakeholders. A lack of social acceptance can terminate technologically and economically promising projects. For that reason, social and environmental aspects need to play a major role in all geothermal development stages. Balancing cultural, social, environmental and economic concerns during geothermal development will enhance and expand utilization of geothermal resources.

Advanced computational methods. Advanced computational methods, including PFA, ML techniques, VOI analysis and 3D conceptual modelling, hold promise for reducing the risks in geothermal drilling and development, particularly in the identification of hidden geothermal resources. Adapted from the petroleum industry[181], geothermal PFA involves integration of geological, geophysical and geochemical parameters indicative of geothermal activity[9,10,182]. PFA by ref.[10] utilized approximately ten features to evaluate heat flow and regional-scale, intermediate-scale and local-scale permeability, which collectively defined the most likely areas for geothermal fluid flow (termed play fairways). Logistic regression, weights of evidence, other statistical measures and expert knowledge were used to gauge weights of influence for each parameter or group of features. However, geothermal PFA faces key challenges, including objectively estimating weights of influence for various features, incomplete datasets, lack of key datasets and limited number of training sites[183]. PFA methodologies can also vary widely depending on geological setting, quality of exposure and effectiveness of geophysical techniques under local conditions[9,182,184]. Although they have only been applied to geothermal systems since the early 2010s, ML techniques can potentially mitigate some of the challenges in PFA and further reduce the risks in geothermal drilling and development. Supervised ML methods involve algorithms optimized to associate pairs of measurable features and labels by utilizing many examples and are applicable to geothermal datasets and exploration. Specific challenges to adapting ML techniques to PFA include customizing techniques to account for multidimensional arrays (tensors) of features distributed on 2D and 3D maps, relatively few training sites and mix of data types (numerical, categorical and ordinal variables).

ML methods have been successfully adapted to complex geological problems[185], and ongoing studies are encouraging for application of ML to PFA[186]. Geothermal suitability distribution was assessed for the first time on a global scale based on 15 interdisciplinary datasets[187] (such as heat flow, groundwater resources, seismic activity and CO_2 emissions). By illustrating global heat flow, major fault zones and active volcanoes together with the spatial distribution of existing geothermal power plants[4] and geological and technological data (Fig. 1), we show the key regions where geothermal resources are currently used for power generation, considering the different power plant technologies (dry steam, single and/or double flash, binary). Global attempts like this highlight the vast potential of geothermal resources and are important for scientific communication to decision makers and the general population, because they inform on the fundamental components of a widely applicable form of renewable energy.

As more data become available for geothermal exploration and development, advanced geostatistical methods grow increasingly important in evaluating individual datasets or features, as well as their relative importance and the associated uncertainties[188]. Advanced geostatistical methods with direct applications to assessing features affecting permeability, stress state or heat source include cluster analysis, principal component analysis, indicator variograms and cokriging. VOI analysis incorporates advanced geostatistical methods, geostatistical modelling and/or ML to provide an objective assessment of which data types and data density are most reliable in identifying productive geothermal wells for a given economic cost[189,190]. VOI analysis can, thus, be used to assess weightings of individual parameters in PFA, optimize new data acquisitions and develop overall exploration strategies.

At the local or prospect scales, integration of 3D geological[191] and geophysical[192] data with the development of resource conceptual models[48] is crucial for selecting the final sites for drilling production and reinjection wells. The 3D geological models constrain multiple parameters that control subsurface permeability and heat, including fault geometries, stress state on faults, basin architecture, stratigraphic framework, rock properties and hydrogeology. 3D modelling of gravity and magnetic data increases certainty that subsurface models are quantitatively consistent with both geological and geophysical data. Conceptual models provide a framework to understand the geological, geochemical, geophysical and geostatistical results in light of thermodynamic constraints, allowing the development of a range of predictions for the spatial distribution of temperature, hydrothermal upflow and outflow pathways, and reservoir geometry and size[48]. Thus, the integration of advanced computational methods into the conceptual modelling process improves well targeting in addition to facilitating quantitative VOI analysis for the evaluation of the relative importance of individual datasets.

Advances in computational methods (such as PFA, ML and VOI analysis) and drilling technologies hold great promise in overcoming challenges in geothermal exploration. Collectively, innovative computational techniques provide an encouraging roadmap to a future in which renewable geothermal energy derived from all types of systems becomes a major component of the global energy budget and notably contributes to the reduction of our carbon footprint. Moreover, the geothermal sector is also gaining attention as an alternative to the oil and gas industry[193], which poses a great opportunity for geothermal developers to benefit from the capital and expertise of the oil and gas sector, and to expand utilization of exploited oil and gas fields for cogeneration.

1. Goldstein, B. et al. in *IPCC Special Report on Renewable Energy Sources and Climate Change Mitigation* Ch. 4 (eds Goodfellow, I., Bengio, Y. & Courville, A.) (MIT Press, 2018).
2. Huttrer, G. W. in *Proceedings of the World Geothermal Congress 2020* (2020).
3. Lund, J. W. & Toth, A. N. Direct utilization of geothermal energy 2020 worldwide review. *Geothermics* **90**, 101915 (2020).
4. ThinkGeoEnergy. Global Geothermal Power Plant Map – updated. *ThinkGeoEnergy.* https://www.thinkgeoenergy.com/map/ (2020).
5. Axelsson, G. Sustainable geothermal utilization – case histories; definitions; research issues and modelling. *Geothermics* **39**, 283–291 (2010).
6. Faulds, J. E. & Hinz, N. H. in *Proceedings of the World Geothermal Congress 2015* (2015).
7. Coolbaugh, M. F., Kratt, C., Fallacaro, A., Calvin, W. M. & Taranik, J. V. Detection of geothermal anomalies using advanced spaceborne thermal emission and reflection radiometer (ASTER) thermal infrared images at Bradys Hot Springs, Nevada, USA. *Remote Sens. Environ.* **106**, 350–359 (2007).
8. Jolie, E., Klinkmueller, M., Moeck, I. & Bruhn, D. Linking gas fluxes at Earth's surface with fracture zones in an active geothermal field. *Geology* **44**, 187–190 (2016).
9. Faulds, J. E. et al. in *Proceedings of the 42nd Workshop on Geothermal Reservoir Engineering* (2017).
10. Faulds, J. E. et al. Searching for blind geothermal systems utilizing play fairway analysis, western Nevada. *Geotherm. Resour. Counc. Bull.* **47**, 34–42 (2018).
11. White, D., Muffler, L. & Truesdell, A. Vapor-dominated hydrothermal systems compared with hot-water systems. *Econ. Geol.* **66**, 75–97 (1971).
12. Hayba, D. O. & Ingebritsen, S. E. Multiphase groundwater flow near cooling plutons. *J. Geophys. Res.* **102**, 12235–12252 (1997).
13. Moeck, I. S. Catalog of geothermal play types based on geologic controls. *Renew. Sustain. Energy Rev.* **37**, 867–882 (2014).
14. Axelsson, G., & Franzson, H. in *Proceedings of the Short Course on Geothermal Development and Geothermal Wells* (2012).
15. Stimac, J., Goff, F. & Goff, C. J. in *The Encyclopedia of Volcanoes* 2nd edn (ed. Sigurdsson, H.) 799–822 (Academic, 2015).
16. Hochstein, M. P. in *Small Geothermal Resources: A Guide to Development and Utilization* Ch. 2 (eds Dickson, M. H. & Fanelli, M.) 31–59 (UNITAR, 1990).
17. Muffler, L. J. P. & Cataldi, R. Methods for regional assessment of geothermal resources. *Geothermics* **7**, 53–89 (1978).
18. Nicholson, K. in *Geothermal Fluids* 1–18 (Springer, 1993).
19. Sanyal, S. K. in *Proceedings of the 13th Workshop on Geothermal Reservoir Engineering* (2005).
20. DiPippo, R. *Geothermal Power Plants: Principles, Applications and Case Studies* 4th edn (Butterworth-Heinemann, 2016).
21. Orenstein, R. & Delwiche, B. The Don A. Campbell geothermal project – development of a low-temperature resource. *Geotherm. Resour. Counc. Trans.* **38**, 91–98 (2014).
22. Mines, G., in *Geothermal Power Generation* Ch. 13 (ed. DiPippo, R.) 353–389 (Woodhead Publishing, 2016).
23. Lucazeau, F. Analysis and mapping of an updated terrestrial heat flow data set. *Geochem. Geophys. Geosyst.* **20**, 4001–4024 (2019).
24. Blackwell, D. D., Negraru, P. T. & Richards, M. C. Assessment of the enhanced geothermal system resource base of the United States. *Nat. Resour. Res.* **15**, 283–308 (2006).
25. Breede, K. et al. A systematic review of enhanced (or engineered) geothermal systems: past, present and future. *Geotherm. Energy* **1**, 4 (2013).
26. Olasolo, P., Juárez, M. C., Morales, M. P. & Liarte, I. A. Enhanced geothermal systems (EGS): a review. *Renew. Sustain. Energy Rev.* **56**, 133–144 (2016).
27. Lu, S.-M. A global review of enhanced geothermal system (EGS). *Renew. Sustain. Energy Rev.* **81**, 2902–2921 (2018).
28. Genter, A., Evans, K., Cuenot, N., Fritsch, D. & Sanjuan, B. Contribution of the exploration of deep crystalline fractured reservoir of Soultz to the knowledge of enhanced geothermal systems (EGS). *C. R. Geosci.* **342**, 502–516 (2010).
29. Cummings, R. G., & Morris, G. E. Economic modeling of electricity production from hot dry rock geothermal reservoirs: methodology and analyses. Final report. (No. EPRI-EA-630; LA-7888-HDR). Dept. of Economics, New Mexico Univ., Albuquerque (USA) http://www.osti.gov/bridge/servlets/purl/5716131-wg4gUV/native/5716131.pdf (1979).
30. Fridleifsson, G. O. & Elders, W. A. The Iceland Deep Drilling Project: a search for deep unconventional geothermal resources. *Geothermics* **34**, 269–285 (2005).
31. Reinsch, T. et al. Utilizing supercritical geothermal systems: a review of past ventures and ongoing research activities. *Geotherm. Energy* **5**, 16 (2017).
32. Ingason, K., Kristjánsson, V. & Einarsson, K. Design and development of the discharge system of IDDP-1. *Geothermics* **49**, 58–65 (2014).
33. Elders, W. A. & Moore, J. N. in *Geothermal Power Generation* Ch. 2 (ed. DiPippo, R.) 7–32 (Woodhead Publishing, 2016).
34. Blackwell, D. D. & Richards, M. *Heat Flow Map of North America* (American Association of Petroleum Geology, 2004).
35. Morgan P. in *Encyclopedia of Solid Earth Geophysics* (ed. Gupta, H. K.) 573–581 (Springer, 2011).
36. Arnórsson, S. Geothermal systems in Iceland: structure and conceptual models — I. High-temperature areas. *Geothermics* **24**, 561–602 (1995).
37. Wilson, C. J. N. & Rowland, J. V. The volcanic, magmatic and tectonic setting of the Taupo Volcanic Zone, New Zealand, reviewed from a geothermal perspective. *Geothermics* **59**, 168–187 (2016).
38. Flóvenz, Ó. G. & Saemundsson, K. Heat flow and geothermal processes in Iceland. *Tectonophysics* **225**, 123–138 (1993).
39. Bibby, H. M., Caldwell, T. G., Davey, F. J. & Webb, T. H. Geophysical evidence on the structure of the Taupo Volcanic Zone and its hydrothermal circulation. *J. Volcanol. Geotherm. Res.* **68**, 29–58 (1995).
40. Blackwell, D. D. in *The Role of Heat in the Development of Energy and Mineral Resources in the Northern Basin and Range Province* (ed. Eaton, G.) 81–93 (Geothermal Resources Council, 1983)
41. Tezcan, A. K. in *Terrestrial Heat Flow and Geothermal Energy in Asia* (eds Gupta, M. L. & Yamano, M.) 23–42 (Oxford and IBH Publishing, 1995).
42. Stelling, P. et al. Geothermal systems in volcanic arcs: volcanic characteristics and surface manifestations as indicators of geothermal potential and favorability worldwide. *J. Volcanol. Geotherm. Res.* **324**, 57–72 (2016).
43. McNamara, D. D. et al. Tectonic controls on Taupo Volcanic Zone geothermal expression: insights from Te Mihi, Wairakei geothermal field. *Tectonics* **38**, 3011–3033 (2019).
44. Minissale, A. The Larderello geothermal field: a review. *Earth Sci. Rev.* **31**, 133–151 (1991).
45. Goldscheider, N., Szonyi, J. M., Eross, A. & Schill, E. Thermal water resources in carbonate rock aquifers. *Hydrogeol. J.* **18**, 1303–1318 (2010).
46. Koçyiğit, A. An overview on the main stratigraphic and structural features of a geothermal area: the case of Nazilli-Buharkent section of the Büyük Menderes Graben, SW Turkey. *Geodin. Acta* **27**, 85–109 (2015).
47. Siler, D. L., Hinz, N. H., Faulds, J. E. & Queen, J. in *Proceedings of the 41st Workshop on Geothermal Reservoir Engineering* (2016).
48. Cumming, W. in *Geothermal Power Generation* Ch. 3 (ed. DiPippo, R.) 33–75 (Woodhead Publishing, 2016).
49. Harvey, C. & Beardsmore, G. (eds) *Best Practices Guide for Geothermal Exploration* 2nd edn (International Geothermal Association, 2014).
50. Björnsson, G. & Bödvarsson, G. A survey of geothermal reservoir properties. *Geothermics* **19**, 17–27 (1990).
51. Lamur, A. et al. The permeability of fractured rocks in pressurized volcanic and geothermal systems. *Nat. Sci. Rep.* **7**, 6173 (2017).
52. Heap, M. J. et al. A multidisciplinary approach to quantify the permeability of the Whakaari/White Island volcanic hydrothermal system (Taupo Volcanic Zone, New Zealand). *J. Volcanol. Geotherm. Res.* **332**, 88–108 (2017).
53. Stimac, G., Nordquist, G., Suminar, A. & Siradz-Azwar, L. An overview of the Awibengkok geothermal system, Indonesia. *Geothermics* **37**, 300–331 (2008).
54. Siratovich, P. A., Heap, M. J., Villenueve, M. C., Cole, J. W. & Reuschlé, T. Physical property relationships of the Rotokawa Andesite, a significant geothermal reservoir rock in the Taupo Volcanic Zone, New Zealand. *Geotherm. Energy* **2**, 10 (2014).
55. McNamara, D. D., Massiot, C., Lewis, B. & Wallis, I. C. Heterogeneity of structure and stress in the Rotokawa Geothermal Field, New Zealand. *J. Geophys. Res.* **120**, 1243–1262 (2015).
56. Stimac, J. A., Powell, T. S. & Golla, G. Porosity and permeability of the Tiwi geothermal field, Philippines, based on continuous and spot core measurements. *Geothermics* **33**, 87–107 (2004).
57. Browne, P. R. L. Hydrothermal alteration in active geothermal fields. *Annu. Rev. Earth Planet. Sci.* **6**, 229–250 (1978).
58. Wyering, L. D. et al. Mechanical and physical properties of hydrothermally altered rocks, Taupo Volcanic Zone, New Zealand. *J. Volcanol. Geotherm. Res.* **288**, 76–93 (2014).
59. Henley, R. W. & Ellis, A. J. Geothermal systems ancient and modern: a geochemical review. *Earth Sci. Rev.* **19**, 1–50 (1983).
60. Sanchez-Alfaro, P. et al. Physical, chemical and mineralogical evolution of the Tolhuaca geothermal system, southern Andes, Chile: Insights into the interplay between hydrothermal alteration and brittle deformation. *J. Volcanol. Geotherm. Res.* **324**, 88–104 (2016).
61. Moore, J. N., Adams, M. C. & Anderson, A. J. The fluid inclusion and mineralogic record of the transition from liquid- to vapor-dominated conditions in The Geysers geothermal system, California. *Econ. Geol.* **95**, 1719–1737 (2000).
62. Glynn-Morris, T., Mclean, K. & Brockbank, K. in *Proceedings of the New Zealand Geothermal Workshop* (2011).
63. Sibson, R. H. Crustal stress, faulting and fluid flow. *Geol. Soc. Lond. Spec. Publ.* **78**, 69–84 (1994).
64. Jentsch, A. et al. Magmatic volatiles to assess permeable volcano-tectonic structures in the Los Humeros geothermal field, Mexico. *J. Volcanol. Geotherm. Res.* **394**, 106820 (2020).
65. Caine, J. S., Evans, J. P. & Forster, C. B. Fault zone architecture and permeability structure. *Geology* **24**, 1025–1028 (1996).
66. Kissling, W. M., Villamor, P., Ellis, S. M. & Rae, A. Modelling of hydrothermal fluid flow and structural architecture in an extensional basin, Ngakuru Graben, Taupo Rift, New Zealand. *J. Volcanol. Geotherm. Res.* **357**, 134–151 (2018).
67. Jolie, E., Hutchison, W., Driba, D. L., Jentsch, A. & Gizaw, B. Pinpointing deep geothermal upflow in zones of complex tectono-volcanic degassing: new insights from Aluto volcano, Main Ethiopian Rift. *Geochem. Geophys. Geosyst.* **20**, 4146–4161 (2019).
68. Curewitz, D. & Karson, J. A. Structural settings of hydrothermal outflow: Fracture permeability maintained by fault propagation and interaction. *J. Volcanol. Geotherm. Res.* **79**, 149–168 (1997).
69. Larson, P. H. Relay structures in a Lower Permian basement-involved extension system, East Greenland. *J. Struct. Geol.* **10**, 3–8 (1988).
70. Childs, C., Watterson, J. & Walsh, J. J. Fault overlap zones within developing normal fault systems. *J. Geol. Soc. Lond.* **152**, 535–549 (1995).
71. Faulds, J. E. & Varga, R. in *Accommodation Zones and Transfer Zones: The Regional Segmentation of the Basin and Range Province* (eds Faulds, J. E. & Stewart, J. H.) 1–46 (Geological Society of America, 1998).
72. Siler, D. L., Hinz, N. H. & Faulds, J. E. Stress concentrations at structural discontinuities in active fault zones in the western United States: Implications for permeability and fluid flow in geothermal fields. *Geol. Soc. Am. Bull.* **130**, 1273–1288 (2018).
73. Micklethwaite, S. & Cox, S. F. Fault-segment rupture, aftershock-zone fluid flow, and mineralization. *Geology* **32**, 813–816 (2004).
74. Faulds, J. E. Structural controls of geothermal activity in the northern Hot Springs Mountains, western Nevada: the tale of three geothermal systems (Brady's, Desert Peak, and Desert Queen). *Geotherm. Resour. Counc. Trans.* **34**, 675–683 (2010).

75. Faulds, J. E., Bouchot, V., Moeck, I. & Oguz, K. Structural controls on geothermal systems in Western Turkey: a preliminary report. *Geotherm. Resour. Counc. Trans.* **33**, 375–381 (2009).
76. Rowland, J. V. & Simmons, S. F. Hydrologic, magmatic, and tectonic controls on hydrothermal flow, Taupo Volcanic Zone, New Zealand: Implications for the formation of epithermal vein deposits. *Econ. Geol.* **107**, 427–457 (2012).
77. Muraoka, H. et al. in *Proceedings of the World Geothermal Congress 2010* (2010).
78. Hulen, J., Kaspereit, D., Norton, D. L., Osborn, W. & Pulka, F. S. Refined conceptual modeling and a new resource estimate for the Salton Sea geothermal field, Imperial Valley, California. *Geotherm. Resour. Counc. Trans.* **26**, 29–36 (2002).
79. Faulds, J. E., Hinz, N. H., Dering, G. M. & Drew, D. L. The hybrid model – the most accommodating structural setting for geothermal power generation in the Great Basin, western USA. *Geotherm. Resour. Counc. Trans.* **37**, 3–10 (2013).
80. Ayling, B. F. in *Proceedings of the 45th Workshop on Geothermal Reservoir Engineering* (2020).
81. Hinz, N. H. et al. in *Proceedings of the 41st Workshop on Geothermal Reservoir Engineering* (2016).
82. Marrett, R. & Allmendinger, R. W. Kinematic analysis of fault-slip data. *J. Struct. Geol.* **12**, 973–986 (1990).
83. Zoback, M. D. et al. Determination of stress orientation and magnitude in deep wells. *Int. J. Rock Mech. Min. Sci.* **40**, 1049–1076 (2003).
84. Davatzes, N. C. & Hickman, S. in *Proceedings of the World Geothermal Congress 2010* (2010).
85. Reiter, K. & Heidbach, O. 3-D geomechanical-numerical model of the contemporary crustal stress state in the Alberta Basin (Canada). *Solid Earth* **5**, 1123–1149 (2014).
86. Ziegler, M. O., Heidbach, O., Reinecker, J., Przybycin, A. M. & Scheck-Wenderoth, M. A multi-stage 3-D stress field modelling approach exemplified in the Bavarian Molasse Basin. *Solid Earth* **7**, 1365–1382 (2016).
87. Barton, C. et al. in *Proceedings of Society of Petroleum Engineers/International Society of Rock Mechanics and Mining Sciences Rock Mechanics in Petroleum Engineering* Vol. 2 315–322 (Society of Petroleum Engineers, 1998)
88. Gaucher, E. et al. Induced seismicity in geothermal reservoirs: a review of forecasting approaches. *Renew. Sustain. Energy Rev.* **52**, 1473–1490 (2015).
89. Evans, K. F., Zappone, A., Kraft, T., Deichmann, N. & Moia, F. A survey of the induced seismic responses to fluid injection in geothermal and CO2 reservoirs in Europe. *Geothermics* **41**, 30–54 (2012).
90. Poux, B., Gunnarsdóttir, S. H. & O'Brien, J. 3-D modeling of the Hellisheiði geothermal field, Iceland, using Leapfrog. *Geotherm. Resour. Counc. Trans.* **42**, 524–542 (2018).
91. Ellis, A. J. & Mahon, W. A. J. *Chemistry and Geothermal Systems* (Academic, 1977).
92. Helgeson, H. C. Geologic and thermodynamic characteristics of the Salton Sea geothermal system. *Am. J. Sci.* **266**, 129–166 (1968).
93. Arnórsson, S., Stefansson, A. & Bjarnason, J. Ö. Fluid-fluid interactions in geothermal systems. *Rev. Mineral. Geochem.* **65**, 259–312 (2007).
94. Craig, H. in *Nuclear Geology on Geothermal Areas* (ed. Tongiori, E.) 17–53 (Spoleto, 1963).
95. Dempsey, D. E., Simmons, S. F., Archer, R. A. & Rowland, J. V. Delineation of catchment zones of geothermal systems in large-scale rifted settings. *J. Geophys. Res. Solid Earth* **117**, B10201 (2012).
96. Delvaux, D. et al. in *Proceedings of the World Geothermal Congress 2010* (2010).
97. Lelli, M. et al. Fluid geochemistry of the Los Humeros geothermal field (LHGF - Puebla, Mexico): new constraints for the conceptual model. *Geothermics* **90**, 101983 (2021).
98. Arnórsson, S. Major element chemistry of the geothermal sea-water at Reykjanes and Svartsengi, Iceland. *Mineral. Mag.* **42**, 209–220 (1978).
99. Giggenbach, W. F. Isotopic shifts in waters from geothermal and volcanic systems along convergent plate boundaries and their origin. *Earth Planet. Sci. Lett.* **113**, 495–510 (1992).
100. Arnórsson, S., Grönvold, K. & Sigurdsson, S. Aquifer chemistry of four high-temperature geothermal systems in Iceland. *Geochim. Cosmochim. Acta.* **42**, 523–536 (1978).
101. Stefánsson, A., Keller, N. S., Robin, J. G. & Ono, S. Multiple sulfur isotope systematics of Icelandic geothermal fluids and the source and reactions of sulfur in volcanic geothermal systems at divergent plate boundaries. *Geochim. Cosmochim. Acta* **165**, 307–323 (2015).
102. 102. Stefánsson, A. et al. Mantle CO2 degassing through the Icelandic crust: evidence from carbon isotopes in groundwater. *Geochim. Cosmochim. Acta* **191**, 300–319 (2016).
103. 103. Wagner, W. et al. IAPWS industrial formulation 1997 for the thermodynamic properties of water and steam. *J. Eng. Gas Turbine Power* **122**, 150–180 (2000).
104. 104. Sourirajan, S. & Kennedy, G. C. The system H2O-NaCl at elevated temperatures and pressures. *Am. J. Sci.* **260**, 115–141 (1962).
105. 105. Ingebritsen, S. & Sorey, M. Vapor-dominated zones within hydrothermal systems: evolution and natural state. *J. Geophys. Res.* **93**, 13,635–13,655 (1988).
106. 106. Allis, R. in *Proceedings of the World Geothermal Congress 2000* (2000).
107. Raharjo, I. B., Allis, R. G. & Chapman, D. S. Volcanohosted vapor-dominated geothermal systems in permeability space. *Geothermics* **62**, 22–32 (2016).
108. 108. Pruess, K. & Narasimhan, T. N. On fluid reserves and the production of superheated steam from fractured, vapor-dominated geothermal reservoirs. *J. Geophys. Res.* **87**, 9329–9339 (1982).
109. 109. Scott, S. W. Decompression boiling and natural steam cap formation in high-enthalpy geothermal systems. *J. Volcanol. Geotherm. Res.* **395**, 106765 (2020).
110. 110. Markusson, S. H. & Stefansson, A. Geothermal surface alteration of basalts, Krýsuvík Iceland — Alteration mineralogy, water chemistry and the effects of acid supply on the alteration process. *J. Volcanol. Geotherm. Res.* **206**, 46–59 (2011).
111. 111. Schiffman, P. & Friðleifsson, G. Ó. The smectite–chlorite transition in drillhole NJ-15, Nesjavellir geothermal field, Iceland: XRD, BSE and electron microprobe investigations. *J. Metamorph. Geol.* **9**, 679–696 (1991).
112. 112. Kristmannsdóttir, H. Alteration of basaltic rocks by hydrothermal activity at 100–300°C. *Dev. Sedimentol.* **27**, 359–367 (1979).
113. 113. D'Amore, F. & Truesdell, A. H. Calculation of geothermal reservoir temperatures and steam fractions from gas compositions. *Geotherm. Resour. Counc. Trans.* **9**, 305–310 (1985).
114. 114. Arnórsson, S., Björnsson, S., Muna, Z. Z. W. & Bwire-Ojiambo, S. The use of gas chemistry to evaluate boiling processes and initial steam fractions in geothermal reservoirs with an example from the Olkaria field, Kenya. *Geothermics* **19**, 497–514 (1990).
115. 115. Scott, S., Gunnarsson, I., Arnórsson, S. & Stefánsson, A. Gas chemistry, boiling and phase segregation in a geothermal system, Hellisheidi, Iceland. *Geochim. Cosmochim. Acta* **124**, 170–189 (2014).
116. 116. Arnórsson, S. & D'Amore, F. in *Isotopic and Chemical Techniques in Geothermal Exploration, Development and Use: Sampling Methods, Data Handling, Interpretation* (ed. Arnórsson, S.) Ch. 9 (International Atomic Energy Agency, 2000).
117. 117. Grant, M. A. Production induced boiling and cold water entry in the Cerro Prieto geothermal reservoir indicated by chemical and physical measurements. *Geothermics* **13**, 117–140 (1984).
118. 118. Corsi, R. Scaling and corrosion in geothermal equipment: problems and preventive measures. *Geothermics* **15**, 839–856 (1986).
119. 119. Gallup, D. L. Geochemistry of geothermal fluids and well scales, and potential for mineral recovery. *Ore Geol. Rev.* **12**, 225–236 (1998).
120. 120. Valdez, B. et al. Corrosion and scaling at Cerro Prieto geothermal field. *Anti-corros. Meth. Mater.* **56**, 28–34 (2009).
121. 121. Scott, S., Driesner, T. & Weis, P. Boiling and condensation of saline geothermal fluids above magmatic intrusions. *Geophys. Res. Lett.* **44**, 1696–1705 (2017).
122. 122. Truesdell, A. H., Haizlip, J. R., Armannsson, H. & Amore, F. D. Origin and transport of chloride in superheated geothermal steam. *Geothermics* **18**, 295–304 (1989).
123. 123. Marini, L., Moretti, R. & Accornero, M. Sulfur isotopes in magmatic-hydrothermal systems, melts, and magmas. *Rev. Mineral. Geochem.* **73**, 423–492 (2011).
124. 124. Kamila, Z., Kaya, E. & Zarrouk, S. J. Reinjection in geothermal fields: an updated worldwide review 2020. *Geothermics* **89**, 101970 (2020).
125. 125. Kristmannsdóttir, H. Types of scaling occurring by geothermal utilization in Iceland. *Geothermics* **18**, 183–190 (1989).
126. 126. Mroczek, E., Graham, D., Siega, C. & Bacon, L. Silica scaling in cooled silica saturated geothermal water: comparison between Wairakei and Ohaaki geothermal fields, New Zealand. *Geothermics* **69**, 145–152 (2017).
127. 127. Ungemach, P. Reinjection of cooled geothermal brines into sandstone reservoirs. *Geothermics* **32**, 743–761 (2003).
128. 128. Capuano, L. E. in *Geothermal Power Generation* Ch. 5 (ed. DiPippo, R.) 107–139 (Woodhead Publishing, 2016).
129. 129. Grant, M. A. & Bixley, P. F. *Geothermal Reservoir Engineering* 2nd edn. (Academic, 2011).
130. 130. Axelsson G., Björnsson, G. & Montalvo, F. in *Proceedings of the World Geothermal Congress 2005* (2005).
131. 131. Axelsson, G. in *Comprehensive Renewable Energy* (ed. Sayigh A.) 3–50 (Elsevier, 2012)
132. 132. Zarrouk, S. J. & Moon, H. Efficiency of geothermal power plants: A worldwide review. *Geothermics* **51**, 142–153 (2014).
133. 133. Sanyal, S. K. & Morrow, J. W. in *Proceedings of the Thirty-Seventh Workshop on Geothermal Reservoir Engineering* (2012).
134. 134. Allen, M. et al. *Success of Geothermal Wells: a Global Study* (International Finance Corporation, 2013).
135. 135. Dobson, P. et al. Analysis of curtailment at The Geysers geothermal Field, California. *Geothermics* **87**, 101871 (2020).
136. 136. Tester, J. W. et al. *The Future of Geothermal Energy: Impact of Enhanced Geothermal Systems (EGS) on the United States in the 21st Century* (MIT Press, 2006).
137. 137. Axelsson, G. & Thórhallsson, S. Review of well stimulation operations in Iceland. *Geotherm. Resour. Counc. Trans.* **33**, 795–800 (2009).
138. 138. Hofmann, H., Zimmermann, G., Zang, A. & Min, K. B. Cyclic soft stimulation (CSS): a new fluid injection protocol and traffic light system to mitigate seismic risks of hydraulic stimulation treatments. *Geotherm. Energy* **6**, 27 (2018).
139. 139. Eggertsson, G. H., Lavallee, Y., Kendrick, J. E. & Markusson, S. H. Improving fluid flow in geothermal reservoirs by thermal and mechanical stimulation: the case of Krafla volcano, Iceland. *J. Volcanol. Geotherm. Res.* **391**, 106351 (2020).
140. 140. Siratovich, P. A., Villeneuve, M. C., Cole, J. W., Kennedy, B. M. & Bégué, F. Saturated heating and quenching of three crustal rocks and implications for thermal stimulation of permeability in geothermal reservoirs. *Int. J. Rock Mech. Min. Sci.* **80**, 265–280 (2015).
141. 141. Morris, A., Ferrill, D. A. & Henderson, D. B. Slip-tendency analysis and fault reactivation. *Geology* **24**, 275–278 (1996).
142. 142. Ferrill, D. A. et al. Stressed rock strains groundwater at Yucca Mountain, Nevada. *GSA Today* **9**, 1–8 (1999).
143. 143. Majer, E. L. et al. Induced seismicity associated with enhanced geothermal systems. *Geothermics* **36**, 185–222 (2007).
144. 144. Zang, A. et al. How to reduce fluid-injection-induced seismicity. *Rock Mech. Rock Eng.* **52**, 475–493 (2019).
145. 145. Kwiatek, G. et al. Controlling fluid-induced seismicity during a 6.1-km-deep geothermal stimulation in Finland. *Sci. Adv.* **5**, eaav7224 (2019).
146. 146. Tarcan, G. Mineral saturation and scaling tendencies of waters discharged from wells (>150 °C) in geothermal areas of Turkey. *J. Volcanol. Geotherm. Res.* **142**, 263–283 (2005).
147. 147. Gunnarsson, I. & Arnórsson, S. Impact of silica scaling on the efficiency of heat extraction from high-temperature geothermal fluids. *Geothermics* **34**, 320–329 (2005).
148. 148. Ölçenoğlu, K. Scaling in the reservoir in Kizildere geothermal field, Turkey. *Geothermics* **15**, 731–734 (1986).
149. 149. Gallup, D. L. Investigations of organic inhibitors for silica scale control in geothermal brines. *Geothermics* **31**, 415–430 (2002).
150. 150. Pambudi, N. A. et al. The behavior of silica in geothermal brine from Dieng geothermal power plant, Indonesia. *Geothermics* **54**, 109–114 (2015).

151. Hirtz, P. N. in *Geothermal Power Generation* Ch. 16 (ed. DiPippo, R.) 443–476 (Woodhead Publishing, 2016).
152. Kruszewski, M. & Wittig, V. Review of failure modes in supercritical geothermal drilling projects. *Geotherm. Energy* **6**, 1–29 (2018).
153. Elders, W. A., Friðleifsson, G. Ó. & Pálsson, B. Iceland Deep Drilling Project: the first well, IDDP-1, drilled into magma. *Geothermics* **49**, 1–128 (2014).
154. Fridleifsson, G. Ó. et al. The Iceland Deep Drilling Project at Reykjanes: Drilling into the root zone of a black smoker analog. *J. Volcanol. Geotherm. Res.* **391**, 106435 (2020).
155. Eichelberger, J. et al. Krafla magma testbed: Understanding and using the magma-hydrothermal connection. *Geotherm. Resour. Counc. Trans.* **42**, 2396–2405 (2018).
156. Muraoka, H. et al. The Japan Beyond-Brittle Project. *Sci. Drill.* **17**, 51–59 (2014).
157. Garcia, J. et al. The Northwest Geysers EGS demonstration project, California: Part 1: characterization and reservoir response to injection. *Geothermics* **63**, 97–119 (2016).
158. Bertani, R. et al. in *Proceedings of the 43rd Workshop on Geothermal Reservoir Engineering* (2018).
159. Jolie, E. et al. in *Proceedings of the 43rd Workshop on Geothermal Reservoir Engineering* (2018).
160. Chambefort, I., Mountain, B., Blair, A. & Bignall, G. in *Proceedings of the 41st New Zealand Geothermal Workshop* (2019).
161. Liebscher, A. & Heinrich, C. A. Fluid–fluid interactions in the Earth's lithosphere. *Rev. Mineral. Geochem.* **65**, 1–13 (2007).
162. Heřmanská, M., Stefánsson, A. & Scott, S. Supercritical fluids around magmatic intrusions: IDDP-1 at Krafla, Iceland. *Geothermics* **78**, 101–110 (2019).
163. Scott, S., Driesner, T. & Weis, P. Geologic controls on supercritical geothermal resources above magmatic intrusions. *Nat. Commun.* **6**, 7837 (2015).
164. Scott, S., Driesner, T. & Weis, P. The thermal structure and temporal evolution of high-enthalpy geothermal systems. *Geothermics* **62**, 33–47 (2016).
165. Ármannsson, H. et al. The chemistry of the IDDP-01 well fluids in relation to the geochemistry of the Krafla geothermal system. *Geothermics* **49**, 66–75 (2014).
166. Scott, S. W. & Driesner, T. Permeability changes resulting from quartz precipitation and dissolution around upper crustal intrusions. *Geofluids* **2018**, 6957306 (2018).
167. Fournier, R. The transition from hydrostatic to greater than hydrostatic fluid pressure in presently active continental hydrothermal systems in crystalline rock. *Geophys. Res. Lett.* **18**, 955–958 (1991).
168. Fournier, R. Hydrothermal processes related to movement of fluid from plastic into brittle rock in the magmatic-epithermal environment. *Econ. Geol.* **94**, 1193–1210 (1999).
169. Watanabe, N. et al. Potentially exploitable supercritical geothermal resources in the ductile crust. *Nat. Geosci.* **10**, 140–144 (2017).
170. Violay, M. et al. An experimental study of the brittle-ductile transition of basalt at oceanic crust pressure and temperature conditions. *J. Geophys. Res. Solid Earth* **117**, B03213 (2012).
171. Violay, M., Gibert, B., Mainprice, D. & Burg, J.-P. Brittle versus ductile deformation as the main control of the deep fluid circulation in oceanic crust. *Geophys. Res. Lett.* **42**, 2767–2773 (2015).
172. Cladouhos, T. T. et al. Results from Newberry Volcano EGS demonstration, 2010–2014. *Geothermics* **63**, 44–61 (2016).
173. Watanabe, N. et al. Hydraulic fracturing and permeability enhancement in granite from subcritical/brittle to supercritical/ductile conditions. *Geophys. Res. Lett.* **44**, 5468–5475 (2017).
174. Watanabe, N. et al. Cloud-fracture networks as a means of accessing superhot geothermal energy. *Sci. Rep.* **9**, 939 (2019).
175. Watanabe, N. et al. Stabilizing and enhancing permeability for sustainable and profitable energy extraction from superhot geothermal environments. *Appl. Energy* **260**, 114306 (2020).
176. Hólmgeirsson, S., Ingólfsson, H. P., Eichelberger, J. & Pye, S. Krafla Magma Testbed (KMT): Engineering challenges of drilling into magma and extracting its energy. *Geotherm. Resour. Counc. Trans.* **42**, 2422–2434 (2018).
177. Coumou, D., Driesner, T. & Heinrich, C. A. The structure and dynamics of mid-ocean ridge hydrothermal systems. *Science* **321**, 1825–1828 (2008).
178. Karason, B., Gudjonsdottir, M. S., Valdimarsson, P., Thorolfsson, G. in *Proceedings of the Thirty-Eighth Workshop on Geothermal Reservoir Engineering* (2013).
179. Hiriart, G., Prol-Ledesma, R. M., Alcocer, S., & Espíndola, S. in *Proceedings of the World Geothermal Congress 2010* (2010).
180. Italiano, F. et al. The Marsili volcanic seamount (southern Tyrrhenian Sea): a potential offshore geothermal resource. *Energies* **7**, 4068–4086 (2014).
181. Doust, H. The exploration play: what do we mean by it? *AAPG Bull.* **94**, 1657–1672 (2010).
182. Lautze, N. C. et al. Play fairway analysis of geothermal resources across the State of Hawaii: 1. Geological, geophysical, and geochemical datasets. *Geothermics* **70**, 376–392 (2017).
183. Faulds, J. et al. in *Proceedings of the 45th Workshop on Geothermal Reservoir Engineering* (2020).
184. Siler, D. et al. Play-fairway analysis for geothermal resources and exploration risk in the Modoc Plateau region. *Geothermics* **69**, 15–33 (2017).
185. Cracknell, M. & Reading, A. Geological mapping using remote sensing data: a comparison of five machine learning algorithms, their response to variations in the spatial distribution of training data and the use of explicit spatial information. *Comput. Geosci.* **63**, 22–33 (2014).
186. Brown, S. et al. Machine learning for natural resource assessment: an application to the blind geothermal systems of Nevada. *Geotherm. Resour. Counc. Trans.* **44**, 920–932 (2020).
187. Coro, G. & Trumpy, E. Predicting geographical suitability of geothermal power plants. *J. Clean. Prod.* **267**, 121874 (2020).
188. Ziegler, M. & Heidbach, O. The 3D stress state from geomechanical–numerical modelling and its uncertainties: a case study in the Bavarian Molasse Basin. *Geotherm. Energy* **8**, 11 (2020).
189. Trainor-Guitton, W. J. et al. The value of spatial information for determining well placement: a geothermal example. *Geophysics* **79**, 27–41 (2014).
190. Trainor-Guitton, W. J., Hoversten, G. M., Nordquist, G. & Intani, R. Value of MT inversions for geothermal exploration: Accounting for multiple interpretations of field data & determining new drilling locations. *Geothermics* **66**, 13–22 (2017).
191. Siler, D. L. et al. Three-dimensional geologic mapping to assess geothermal potential: examples from Nevada and Oregon. *Geotherm. Energy* **7**, 2 (2019).
192. Scott, S. W. et al. A probabilistic geologic model of the Krafla geothermal system constrained by gravimetric data. *Geotherm. Energy* **7**, 29 (2019).
193. Ball, P. J. Macro energy trends and the future of geothermal within the low-carbon energy portfolio. *J. Energy Resour. Technol.* **143**, 010904 (2020).
194. Beaulieu, S. E. & Szafranski, K. InterRidge Global Database of Active Submarine Hydrothermal Vent Fields, Version 3.4. http://vents-data.interridge.org (2020).
195. Styron, R. GEMScienceTools/gem-global-active-faults: First release of 2019 (Version 2019.0). *Zenodo* https://doi.org/10.5281/zenodo.3376300 (2019).
196. American Geological Institute. Global GIS: volcanoes of the world; volcano basic data. *EarthWorks, Stanford University* https://earthworks.stanford.edu/catalog/harvard-glb-volc (2020).
197. GEBCO Compilation Group. GEBCO 2020 Grid. *British Oceanographic Data Centre* https://doi.org/10.5285/a29c5465-b138-234d-e053-6c86abc040b9 (2020).
198. Wilmarth, M. & Stimac, J. Power density in geothermal fields. *Power* **19**, 25 (2015).
199. Grant, M. A. in *Proceedings of the World Geothermal Congress 2000* (2000).
200. Wohletz, K. & Heiken, G. *Volcanology and Geothermal Energy* (Univ. California Press, 1992).
201. Muffler, L. J. P. *Assessment of Geothermal Resources of the United States - 1978* (U.S. Geological Survey, 1979).
202. Bohnsack, D., Potten, M., Pfrang, D., Wolpert, P. & Zosseder, K. Porosity–permeability relationship derived from Upper Jurassic carbonate rock cores to assess the regional hydraulic matrix properties of the Malm reservoir in the South German Molasse Basin. *Geotherm. Energy* **8**, 1–147 (2020).
203. Cant, J. L., Siratovich, P. A., Cole, J. W., Villeneuve, M. C. & Kennedy, B. M. Matrix permeability of reservoir rocks, Ngatamariki geothermal field, Taupo Volcanic Zone, New Zealand. *Geotherm. Energy* **6**, 2 (2018).
204. Coulomb, C. A. Essai sur une application des regles des maximis et minimis a quelquels problemesde statique relatifs, a la architecture. *Mem. Acad. Roy. Div. Sav.* **7**, 343–387 (1776).
205. Terzaghi, K. *Theoretical Soil Mechanics* (Wiley-Blackwell, 1943).
206. Milora, S. L. & Tester, J. W. *Geothermal Energy as a Source of Electric Power* (MIT Press, 1976).

Acknowledgements
We are especially grateful to the entire ThinkGeoEnergy team for access to the updated global geothermal power plant database, F. Lucazeau for providing a modified dataset on continental heat flow and E. Trumpy for discussing the global geothermal suitability distribution map.

Author contributions
E.J. developed the concept and structure of the manuscript. All authors contributed to the scientific input, writing and editing of the manuscript.

Competing interests
The authors declare no competing interests.

Peer review information
Nature Reviews Earth & Environment thanks P. G. Ranjith, D. Elsworth and C. Dezayes for their contribution to the peer review of this work.